DISCUSSION PAPER SERIES

No. 9277

CONFLICT, CLIMATE AND CELLS: A DISAGGREGATED ANALYSIS

Mariaflavia Harari and Eliana La Ferrara

DEVELOPMENT ECONOMICS and PUBLIC POLICY

Centre for Economic Policy Research

www.cepr.org

Available online at: **www.cepr.org/pubs/dps/DP9277.asp**

ISSN 0265-8003

CONFLICT, CLIMATE AND CELLS: A DISAGGREGATED ANALYSIS

Mariaflavia Harari, Massachusetts Institute of Technology (MIT)
Eliana La Ferrara, Bocconi University, IGIER and CEPR

Discussion Paper No. 9277
January 2013

Centre for Economic Policy Research
77 Bastwick Street, London EC1V 3PZ, UK
Tel: (44 20) 7183 8801, Fax: (44 20) 7183 8820
Email: cepr@cepr.org, Website: www.cepr.org

CEPR Discussion Paper No. 9277

January 2013

ABSTRACT

Conflict, Climate and Cells: A Disaggregated Analysis*

We conduct a geographically and temporally disaggregated empirical analysis of civil conflict at the sub-national level in Africa over the period 1997-2011. Our units of observation are cells of 1 degree of latitude by 1 degree of longitude. We exploit within-year variation in the timing of weather shocks and in the growing season of different crops, as well as spatial variation in crop cover, to construct an original measure of shocks that are relevant for agricultural production. Employing a new drought index we show that negative climate shocks which occur during the growing season of the main crop cultivated in the cell have a sizeable and persistent effect on conflict incidence. We also use state-of-the-art spatial econometric techniques to test for the presence of temporal and spatial spillovers in conflict, and we find both to be sizeable and highly statistically significant. Exploiting variation in the type of conflict episode, we find that the impact of climate shocks on conflict is particularly significant when focusing on outcomes such as battles and violence against civilians. Our estimates can be used to predict how future warming scenarios affect the prevalence and diffusion of conflict.

JEL Classification: O12
Keywords: Africa, civil conflict, gridded data, spatial and weather shocks

Mariaflavia Harari
Massachusetts Institute of Technology
50 Memorial Drive
E52-391
Cambridge, MA 02142
USA

Email: harari@mit.edu

For further Discussion Papers by this author see:
www.cepr.org/pubs/new-dps/dplist.asp?authorid=176727

Eliana La Ferrara
IGIER
University of Bocconi
Via Sarfatti, 25
20136 Milano
ITALY

Email: eliana.laferrara@unibocconi.it

For further Discussion Papers by this author see:
www.cepr.org/pubs/new-dps/dplist.asp?authorid=145220

*We thank Arun Chandrasekhar, Melissa Dell and Rene Gommes for helpful comments and discussions, Gordon Hughes and Solomon Hsiang for making available their code, seminar participants at MIT, Sciences Po, the Stockholm Climate Economy Conference and the B-WGAPE meeting. Marta Barazzetta, Barbara Biasi, Emanuele Colonnelli, Nicola Fontana, Ludovica Gazze , Selene Ghisol, Simone Lenzu, Anna Martinolli, Edoardo Teso provided excellent research assistance. La Ferrara acknowledges financial support from the European Research Council grant ERC-2007-StG-208661. The usual disclaimer applies.

Submitted 11 December 2012

1 Introduction

Since the publication of the Fourth Assessment Report of the Intergovernmental Panel on Climate Change in 2007, a vivid debate has emerged on the consequences that warming and the increased frequency of extreme weather events have on aggregate economic and geopolitical scenarios. There is particular concern that the adverse impact of these climatic changes may be more strongly felt in areas that have lower capacity for adaptation, typically poorer and politically unstable. Sub-Saharan Africa is one such area. The vast majority of the population in this region is dependent on rainfed agriculture, and estimates of aggregate yield changes for the five main rainfed crops in the region range between -8% and -22% over the next fifty years in response to projected climate change.[1]

Sub-Saharan Africa is also the region that has been most severely affected by violent conflict in the past half century: of the 127 civil wars that occurred between 1945 and 1999, 74 were in Sub-Saharan Africa. The correlation between poverty and vulnerability to weather shocks on one side, and propensity to conflict on the other, has spurred a growing amount of research trying to establish a causal link from the former to the latter.[2] This literature typically employs cross country panel data on precipitation and temperature to estimate how they affect the occurrence of civil war, defined according to predetermined thresholds in the number of deaths per year due to conflict.

In this paper we attempt to make a step further in understanding the relationship between climate and civil conflict by taking the analysis to a different scale. We conduct a geographically disaggregated analysis which takes as units of observation 110 x 110 km subnational "cells", and we estimate the incidence of conflict in a cell as a function of weather shocks and a number of other covariates both in the cell and in neighboring areas, plus a "lag" in space and time of the endogenous variable. The disaggregation thus concerns both the climate indicators, which are measured at the cell level, and the conflict outcomes, which include events of different intensity that can be located in space. This is particularly important when studying the role of climate change, as it is plausible that some of the effects of the latter will be on localized, low intensity conflict.

Our approach contributes to the existing literature in three directions. The first is methodological. We disaggregate the level of analysis both in space and time, constructing a cell-year panel with a rich set of georeferenced covariates. We model spatial and temporal dependence thorough state-of-the-art spatial econometrics techniques which have seldom been applied in economics. In particular, we estimate a model that in-

[1] Schlenker and Lobell (2010).

[2] Starting with the seminal contribution of Miguel et al. (2004), this litarature includes among others Ciccone (2011), Burke et al. (2009), and Buhaug (2010).

cludes spatially and temporally autoregressive terms to account for the fact that conflict may be persistent over time, and that both the covariates and the presence of conflict may be correlated across space. As we explain in the next section, this poses a number of challenges for estimation and constitutes an original contribution to the empirical conflict literature, and one which is particularly crucial when dealing with highly disaggregated data. In terms of results, this disaggregated approach is useful for two reasons. The first is the assessment of how persistent the effects are in space and time: persistence will imply that even temporary shocks may have long lasting effects on political instability. The second is the ability to better detect the presence of conflict spillovers across locations compared to the existing cross country literature.[3] In fact it is arguably more difficult for a civil war to "spill over" to a different country than for a riot or a localized episode of violence to spill over to a neighboring village or town. The disaggregated level of observation also allows us to take a closer look at a number of geographic covariates, which have been claimed to be predictors of conflict but which have so far been measured at a possibly wrong scale.

A second contribution of our paper is that we look at climate indexed *within* the year. Because the main channel linking weather shocks and conflict operates through shocks to agricultural incomes, we attempt to isolate the component of annual climate variability which is relevant for agriculture. In other words, instead of using climate indicators aggregated over the whole year (e.g., average yearly rainfall), we construct specific indicators for climatic conditions during the growing season, which is when crops are most sensitive to unfavorable conditions. This is a data intensive process as it requires a number of steps: identifying the main crop cultivated in each cell; finding the growing season of this crop (which varies across cells); and matching this information with high frequency weather data. In other words, we exploit both within-year variation in the timing of weather shocks as well as spatial variation in crop cover to construct an original measure of agriculture-relevant weather shocks. Once we isolate the impact of the weather shock component which effectively affects local agriculture, we find evidence that this is what drives the overall observed local negative relationship between conflict episodes and weather: shocks occurring outside the growing season have no impact. This is important because it allows us to shed more light on the channel through which climate change may operate, namely shocks to agricultural output and incomes and not generic effects on crime, health, or productivity in non-agricultural sectors.[4]

A third contribution relates to the climate indicator we employ. While most of the conflict literature so far has focused on precipitation (and to a lesser extent on

[3] See for example Buhaug and Gleditsch (2008).

[4] See for example Larrick et al. (2011).

temperature), we use a multiscalar drought index that accounts for the fact that the impact of rainfall on the growing cycle of a plant depends on the extent to which water can be retained by the soil. This in turn depends on the characteristics of the soil and on the extent to which sunshine induces evaporation. The climate indicator we use in our benchmark specification, the Standardized Precipitation-Evapotranspiration Index (SPEI), has been recently developed by Vicente-Serrano et al. (2010) and considers the joint effects of precipitation, potential evaporation and temperature.

Our methodology and results can be summarized as follows. We assemble a panel dataset covering about 2,700 cells in 46 African countries over the period 1997-2011. We combine georeferenced conflict data from the Armed Conflict Location and Event (ACLED) dataset with an originally constructed measure of SPEI plus a large set of cell level covariates. Using maximum likelihood we estimate the probability that a given cell experiences at least one conflict event during the year as a function of cell level covariates, contemporaneous and lagged shocks to SPEI, and spatial and temporal lags of conflict itself. We find that:

(i) There is a significant local-level relationship between agriculture-relevant weather shocks and civil conflict. A spell of SPEI that is one standard deviation below the mean throughout the growing season is associated with a 4 percentage point increase in conflict likelihood in the subsequent year and in the year following that; this is roughly one fourth of the mean of dependent variable.

(ii) Conflict exhibits high persistence both in time and across space. Cells experiencing conflict in a given year have a 33 percentage points higher probability of experiencing it the following year. When a cell experiences conflict, each of its neighboring cells has a 4 percentage points higher probability of experiencing it during the same year. The magnitude of the effect of conflict in another cell is found to decrease with the distance of the cell from the one under consideration, as one would expect.

(iii) Weather shocks to neighboring cells do not seem to have an independent effect on a cell's likelihood of conflict, aside from the effect that is mediated by conflict in the neighboring cells themselves. The impact of weather shocks seems thus to be strictly local: negative shocks increase the probability of future conflict in the cell where they occur, but then this conflict spills over to neighboring cells. This seems to suggest that small, one-time shocks can have potential far-reaching effects through conflict's propensity to propagate.

(iv) Climatic conditions outside the months of the growing season have zero effect on conflict. This suggests that the mechanisms operates through low agricultural yields.

(v) Drawing upon the rich disaggregation of conflict events of the ACLED dataset, we can also look at individual types of conflict episodes. We find a significant effect

of weather shocks on battles, violence against civilians and riots, while the effect is not significant on activities such as rebel recruitment and the establishment of headquarters. This may run counter the theories which emphasize fluctuations in the opportunity cost of joining a civil conflict, but it may also be driven by more pronounced measurement error in recording this type of conflict activities.

(vi) Finally, among time-invariant local characteristics, elevation, terrain ruggedness, road infrastructure, ethno-linguistic fractionalization and the presence of mineral resources are all strong local conflict predictors.

Before proceeding, two caveats are in order. The first is that by focusing on the role of shocks at the local level our paper has very little to say about long term institutional causes of conflict, e.g. those related to the political system. This does not reflect a judgement on the relative importance of the two sets of causes, but is a consequence of the scale at which we conduct our analysis: we believe that aggregate institutional causes are better understood through country level analysis than at the high resolution at which we operate.

The second caveat relates to the extent to which our results speak only to the effects of weather shocks or can say something about the effects of climate change. It should be noted that the main indicator we use in our analysis is not the deviation of SPEI one year to the next, but rather the deviation of SPEI from its long term historical average (or more precisely, the fraction of growing season months in which this deviation is at least one standard deviation below the mean). This indicator can to some extent capture global trends (and it is in fact more negative in more recent years). At the same time, our regression analysis holds constant a number of economic and political variables that may endogenously evolve over the long run: we would thus refrain from extrapolating the results too far into the future, and more generally to contexts where ample possibilities for adaptation exist.

With this caveat in mind, in the last part of the paper we use cell-level projections of future temperature and precipitation for 2012-2030, drawn from the CORDEX Archive (Hernández-Díaz et al., forthcoming), to construct a forecast of our SPEI based indicator. We find that, other things equal, warming sharply increases the frequency of extreme weather events like the ones on which our regression analysis is based. We predict that shocks to SPEI occurring during the growing season, as per definition of our main explanatory variable, will be roughly twice as frequent during the next 20 years. Based on our parameter estimates, this implies that the marginal contribution of future SPEI shocks to conflict incidence in an average cell and year during 2012-2030 is 7 percentage points. As a benchmark, average conflict incidence in during 1997-2011 was .17, i.e. the average cell had a .17 probability of experiencing a conflict event during 1997-2011. The predicted impacts of future warming on conflict incidence is thus quite sizeable.

Our work is related to three strands of literature. The first is the literature on climate and violent conflict. Miguel et al. (2004) were the first to highlight a relationship between rainfall driven economic shocks and conflict incidence in Sub Saharan Africa. Recently, a number of papers (e.g., Ciccone, 2011) have reconsidered the link between rainfall and conflict, indicating that mean-reverting properties and the spatial correlation in rainfall have not been taken into account. Our paper is indeed an attempt to take these factors into consideration conducting the analysis at a more disaggregated level, as well as isolating the component of weather variation that occurs during growing season. At the same time, differently from the above authors who adopt an instrumental variables strategy, we estimate a reduced form relationship - there is no data on income or GDP that varies at yearly frequency and is available at the level of disaggregation that we employ.

Another contribution linking climate to conflict is that of Burke et al. (2009), recently revisited by Buhaug (2010). They estimate the historical relationship between temperature changes and civil war across African countries and combine their estimates with climate model projections of future temperature, predicting large increases in conflict driven by global warming by 2030. Hsiang et al. (2011) also find that conflicts in tropical regions are substantially more likely during hot and dry *El Niño* years than during the cooler *La Niña* years. We share with this literature the acknowledgement that temperature increases are a crucial factor to consider, and indeed our SPEI measure combines data on temperature (which affects evapotranspiration) with data on precipitation. Again, the focus of our work is different in that we employ a different scale and we allow for conflict spillovers in space and time, spillovers which possibly amplify the effects of climate shocks.

Our focus on within country variation is shared by two recent studies. Dell (2012) finds a strong relationship between drought severity and insurgency across municipalities during the Mexican Revolution. Vanden Eynde (2011) uses district level data for India during 2005-2010 and finds that negative rainfall shocks lead to increased Naxalite violence against civilians. We view our large-N, cross cell analysis as complementary to these in depth quantitative case studies.

A second strand of the literature related to our work is that on climate and development. Motivated by the debate on the economic consequences of global warming, recent studies have looked at the impact of temperature on economic activity. Dell, Jones and Olken (2012) find that higher temperatures substantially reduce economic growth in poor countries. Burgess et al. (2011) study how weather shocks impact mortality in India by looking at high frequency variations in rainfall and temperature and conclude that only shocks occurring after the monsoon are relevant. Kudamatsu, Persson and Strömberg (2012) explore a related question with African data and conclude that weather shocks

had a significant impact on child mortality through the channels of malaria and malnutrition. Maccini and Yang (2009) examine the effect of weather shocks around the time of birth on adult age outcomes in Indonesia and find that higher early-life rainfall leads to improved health, schooling, and socioeconomic status for women. In addition to economic and health effects, weather shocks have also been shown to have long lasting impact on countries' political institutions: Brückner and Ciccone (2011) show that negative rainfall shocks increase democracy scores as well as the likelihood of democratic transitions in Africa.

The third and last strand of literature related to our work is that on the determinants of civil conflict. This vast literature includes early cross country empirical work by Collier and Hoeffler (1998) and Fearon and Laitin (2003). Theoretical foundations for the impact of economic shocks have been offered by Dal Bo and Dal Bo (2011) and Chassang and Padro-i-Miquel (2009), and nicely tested by Dube and Vargas (forthcoming). More recently, increasing attention has been devoted to understanding long run institutional determinants of conflict, notably historical conflicts and ethnic partitions, using georeferenced data similar to the ones we use, e.g. by Besley and Reynal-Querol (2012) and Michalopoulos and Papaioannou (2012).

The remainder of the paper is organized as follows. In Section 2 we present our conceptual framework and econometric methodology. In Section 3 we document our data sources and dataset construction and we provide some descriptive statistics on the variables of interest. In Section 4 we discuss the econometric evidence at the cross-sectional (cross-cell) level; while in Section 5 we conduct the main analysis exploiting both cross-sectional and time variation, and focusing on weather shocks. Section 6 concludes.

2 Conceptual framework and methodology

2.1 Conceptual framework

The economic literature on the effects of economic shocks on conflict has traditionally stressed two channels working in opposite directions (see e.g., Collier and Hoeffler, 1998). On the one hand, there is an "opportunity cost" effect: a negative shock to the local economy decreases the returns from labor market participation and productive activity relatively to the returns from fighting, making it relatively more attractive for the local population to join rebellion. On the other hand, the same negative shock implies that the size of the "pie" to be appropriated is also lower, thus reducing the incentives to fight in the first place. The net effect is theoretically ambiguous, and would depend

among other things on whether control of the territory may yield long term economic benefits (e.g., if it is mineral rich) aside from the short term gains appropriated. The fact that the shock occurs to a labor intensive or capital intensive sector also matters. In our case, because African agriculture is typically labor intensive, based on Dal Bo and Dal Bo (2011) the opportunity cost effect would be predicted to prevail compared to the size of the disputable wealth effect, so that negative shocks should lead to more conflict. Economic shocks may also have an additional effect, namely worsening the extent of poverty and exacerbating existing inequalities, thus fueling conflict in response to "grievances".

A different channel has been proposed by Fearon and Laitin (2003), who stress the role of state capacity and infrastructure. To the extent that economic shocks may reduce the tax base from which the government gets its revenue, this would weaken the government's ability to fight rebellion, leading to higher conflict levels. Also, if economic shocks affect the quality of infrastructure (e.g., roads), the increase in conflict may be the result of government's logistical difficulties in repressing insurgents.

As will be clear in the next section, the way in which we construct our shock variable allows us to isolate effects that are specific to agricultural yields. Weather shocks outside the growing season should impact road quality, hence increase conflict likelihood if the main channel were infrastructure. But we find that only shocks that occur during the growing season matter, thus reinforcing the first set of interpretations. As for the revenue channel, the highly disaggregated scale at which we conduct our estimation makes it difficult to capture this type of effect, as total state revenue would be dependent on national economic conditions and not strictly local ones.

2.2 Empirical strategy

To implement our empirical exercise, we construct a dataset that has the structure of a raster grid: the cross-sectional units of observation are subnational "cells" of 1 degree of latitude x 1 degree of longitude, whose sides are placed in correspondence of integer values of latitude and longitude. At these latitudes, 1 degree corresponds on average to approximately 110 km. This "grid" approach is followed, among others, by Alesina, Giuliano and Nunn (2011) and Michalopoulos (2012). An alternative way to conduct a subnational analysis would be to consider administrative units. However, the way in which a country is split into administrative units is in itself the outcome of a political decision: it may take into account both geographical and demographic features of the territory which could all be arguably determinants of conflict themselves, or jointly determined with it. The supposed advantage of using administrative units is that data on income, population or inequality are often available at the administrative level;

however, such variables are almost inevitably endogenous to conflict and incorporating them in a conflict regression is at least problematic. Our approach is one which takes as unit of observation an entity whose borders are truly exogenous to conflict, by ideally superimposing a grid of equally-sized cells on the territory of interest.[5]

The bulk of our empirical analysis is conducted at the cell/year level. Our main dependent variable is ANY EVENT, a binary measure of conflict incidence indicating whether the cell has experienced a conflict-related episode - of any of the categories included in the ACLED dataset - over the course of the year. In order to investigate the local level relationship between climate and conflict incidence we estimate three models. The first is a model containing only exogenous regressors specific to the cell. The second model includes a "spatial lag" of the exogenous regressors, to allow for the possibility that local level variables may directly affect conflict in neighboring areas. The third (preferred) model is one that includes lags of the endogenous variable in time and space, to allow for persistence in time and conflict spillovers across localities.

Model I

Consider a panel of N cells indexed by c, and T years indexed by t. Denote with C a generic climate indicator (e.g., precipitation) and with GS_C the climate indicator measured in the cell-specific growing season (see below). Let X be a vector of controls with no time variation - such as terrain characteristics, and γ and μ denote year and country fixed effects, respectively. Model I takes the following form:

$$ANY\ EVENT_{c,i,t} = \alpha + \sum_{k=0}^{2} \beta_{1k} C_{c,t-k} + \sum_{k=0}^{2} \beta_{2k} GS\_C_{c,t-k} + \delta X_c + \gamma_t + \mu_i + \varepsilon_{c,i,t} \quad (1)$$

where c denotes the cell, i the country and t the year. This specification is essentially the transposition of state-of-the-art cross country conflict regression equations - à la Ciccone (2011) - at a high spatial resolution.

Our dependent variable is binary and several conflict regressions in the literature using a binary dependent variable resort to logit estimators. However, we prefer to conduct the estimation by OLS, thus fitting an unrestricted linear probability model. The reason is twofold. On the one hand, this can be easily integrated with state-of-the-art spatial econometrics techniques, which so far have not been explicitly developed for limited dependent variables. On the other hand, it has been argued that when dealing

[5] One potential difficulty arising when such units of observations are used is the so-called "Modifiable Aeral Unit Problem" (MAUP). We address this issue in section 5.2.

with "rare events", such as wars, logit and probit may yield biased estimates (King and Zheng, 2001).

One key feature of our data is spatial correlation. Most empirical work in the conflict literature implicitly assumes that observations are independent across space, and thus does not take spatial correlation nor spatial dependence into account. When dealing with georeferenced, cross-sectional data with potential spatial dependence the majority of the development literature performs OLS estimation with Conley (1999) standard errors, which are robust to spatial dependence of unknown form in the error term. We estimate Model I by OLS and we apply such a correction to our standard errors, following the procedure of Hsiang (2010) and adjusting standard errors for both spatial and serial correlation.

This is appropriate in cases in which spatial correlation is present in the error term ("spatial error model"), however it does not address the issue of how to explicitly model spatial dependence in the process itself. We expect spatial correlation to be present both in the georeferenced covariates – for example, mineral deposit presence or climatological events – and in conflict itself, through direct cross-cell spillovers.

Model II

A simple way of controlling for spatial correlation in the covariates is to include spatial lags of the variables of interest, just as in time series it is common to include temporal lags. In spatial econometrics the structure of spatial dependence between observations is defined through a symmetric weighting matrix W, and the spatial lag of a given variable is obtained multiplying the matrix W by the vector of observations. Let C_t and GS_C_t be N-dimensional vectors of climate observations in year t, and let X be the matrix of cell-level controls. We estimate Model II:

$$ANY\ EVENT_{c,i,t} = \alpha + \sum_{k=0}^{2} \beta_{1k} C_{c,t-k} + \sum_{k=0}^{2} \beta_{2k} GS\_C_{c,t-k} + \delta X_c + \mu_i + \tag{2}$$

$$+ \sum_{k=0}^{2} \theta_{1k} W \cdot C_{t-k} + \sum_{k=0}^{2} \theta_{2k} W \cdot GS\_C_{t-k} + \lambda W \cdot X + W \cdot \mu + \gamma_t + \varepsilon_{c,i,t}$$

This is a spatial Durbin model (Anselin, 1998) in which we let conflict in one cell depend on covariates observed not only in the cell itself, but also in the neighboring cells. Since the structure of spatial dependence is not directly estimated but assumed, the choice of the weighting matrix is important. A popular choice is that of a binary contiguity

matrix in which a weight of 1 is assigned to cells surrounding the cell of interest - within a given distance cutoff -, and a weight of 0 to other cells. Our benchmark connectivity matrix is a binary matrix with distance cutoff set to 180 km. Because 180 km is the radius of the circle drawn around the cell's center, and each cell is a square with sides of approximately 110 km, this connectivity matrix implies that we effectively consider as neighbors of a given cell the 8 bordering cells. In Section 5 we discuss our choice of the weighting matrix and we conduct a sensitivity analysis to different spatial matrices.

For ease of interpretation we do not row standardize the matrix W, so the coefficients on the spatial lags, θ_{1k}, θ_{2k} and λ, should be interpreted as the effect of a marginal change in the given variable in *one* of the neighbors of each cell. This model has the advantage of simplicity, since including spatial lags of the independent variables is straightforward and poses no particular econometric concerns. Standard errors are corrected for spatial and temporal correlation à la Hsiang (2010).

Model III

We expect spatial correlation to be present not only in the covariates, but also in conflict itself. Allowing for spatial autocorrelation in the dependent variable, in order to capture direct conflict spillovers, is more problematic than allowing for spatial correlation in the controls due to an obvious simultaneity problem. Part of the observed spatial correlation in conflict location is to be attributed to the fact that conflict determinants are spatially correlated themselves; part of it, on the other hand, is to be attributed to direct contagion effects. Disentangling these two effects is in general difficult, as it is a version of the well-known reflection problem (Manski, 1993). Models allowing for spatial dependence in the dependent variable are known as spatial autoregressive models. They have been mostly developed for cross-sectional analysis, and have only recently been extended to panel data (LeSage & Pace, 2009; Elhorst, 2009 among others). These models are estimated with maximum likelihood or GMM techniques and tend to be computationally intensive.

A further complication arises in our context, since in addition to spatial autocorrelation we expect the process of conflict to be autocorrelated in time as well. To fully incorporate both sources of autocorrelation we estimate Model III:

$$ANY\ EVENT_{c,i,t} = \phi ANY\ EVENT_{c,i,t-1} + \rho W \cdot ANY\ EVENT_t + \tag{3}$$

$$\alpha + \sum_{k=0}^{2} \beta_{1k} C_{c,t-k} + \sum_{k=0}^{2} \beta_{2k} GS\_C_{c,t-k} + \delta X_c + \mu_i +$$

$$+\sum_{k=0}^{2}\theta_{1k}W\cdot C_{t-k}+\sum_{k=0}^{2}\theta_{2k}W\cdot GS\_C_{t-k}+\lambda W\cdot X+W\cdot\mu$$

$$+\gamma_t+\varepsilon_{c,i,t}.$$

This is a dynamic, spatially autoregressive Durbin model (Elhorst, 2009) in which we let conflict in one cell depend on lagged conflict in the cell itself, on contemporaneous conflict in the neighboring cells, on covariates in the cell itself and on covariates in the neighboring cells. To our knowledge, this is the first time a spatio-temporal autoregressive model is applied in the empirical conflict literature.

An obvious identification challenge is posed by the endogeneity of the first two regressors, which requires these models to be estimated either by GMM or maximum likelihood. We use the routines developed by Hughes (2012), which are based on quasi-maximum likelihood techniques described in Elhorst (2009) and Parent and LeSage (2009). In particular, we fit a random effects model estimated applying the full maximum likelihood method described in Parent and Le Sage (2009), which treats the value of the dependent variable for the initial time period as exogenous and uses the data for $t = 2, \ldots T$ in the estimation (see the Appendix for details). Standard errors are clustered by cell.

The explicit inclusion of spatially and temporally autoregressive terms represents an innovation of our paper in the empirical literature on conflict, and one which is particularly crucial when dealing with highly disaggregated data. Neglecting spatial patterns has the potential of introducing a serious bias in one's estimates. One possibility is to simply ignore the explicit spatial autoregressive component and estimate the model via plain, non-spatial OLS. This leads to omitted variable bias: the impact of location-specific factors tends to be overestimated as interdependency effects are neglected. Thus, if we limited our analysis to Model I, we might worry that the local impact of climate is driven simply by the fact that conflict is clustered in space and so are climate shocks. A possibility is to explicitly include the spatial autoregressive component and estimate the model via OLS: estimates will suffer simultaneity bias, as the spatial lag will be endogenous. The analyses will be biased in the opposite direction: in the typical case of positive interdependence and positive covariance of spatial lag and exogenous regressors, one would overestimate the interdependence effects and underestimate contextual (cell-specific) effects. This discussion suggests that inference from studies which do not address spatial dependence at all should be taken with caution, especially when considering data at higher geographic resolutions.

Since our focus is on within-country variation in the incidence of conflict, our speci-

fication of choice includes country fixed effects[6], so as to account for long-run aspects of the political, economic or social structure of the states in our sample, as well as for state-level geographic features (e.g. country size). According to Besley and Persson (2008) "this gets around one of the key worries in the literature, namely that it is unobserved characteristics of institutions, culture and economic structure that are primarily responsible for civil war" and ensures that estimation results are not driven by unmeasured features of states. Through the inclusion of year fixed effects we control for global trends in conflict incidence as well as climate.

Cross sectional models

As a preliminary step to our panel analysis, we collapse our cell-year panel to create a time-invariant measure of conflict prevalence in a given cell. Our aim is that of investigating cross-sectional relationships with various local terrain characteristics. Our dependent variable capturing average conflict incidence over time is the fraction of years in the sample in which the cell has experienced at least one conflict event. The aim of the cross-sectional analysis is to highlight geographic correlates of conflict exploiting the high spatial resolution of the dataset to detect these patterns at the appropriate scale. Again, we estimate three models:

$$\overline{ANY\ EVENT}_{c,i} = \alpha + \delta X_c + \mu_i + \varepsilon_{c,i} \tag{4}$$

$$\overline{ANY\ EVENT}_{c,i} = \alpha + \delta X_c + \lambda W \cdot X + W \cdot \mu + \varepsilon_{c,i} \tag{5}$$

which are estimated by OLS with Conley errors, and

$$\overline{ANY\ EVENT}_{c,i} = \alpha + \varphi W \cdot \overline{ANY\ EVENT} + \delta X_c + \lambda W \cdot X + W \cdot \mu + \varepsilon_{c,i} \tag{6}$$

estimated by maximum likelihood with errors clustered by cell.

[6]For the purposes of defining country fixed effects, each cell in the dataset is uniquely assigned to a country. Cells shared among more than one country are assigned to the country which has the largest share of the cell's territory; a "shared" dummy for those cells is also included among the controls.

3 Data

3.1 Sources and dataset construction

We bring together high-frequency, georeferenced data from a variety of sources and construct a dataset which covers 46 African countries over the period 1997-2011[7], including information on individual conflict episodes and on a large number of geo-climatic characteristics. In particular, we collect detailed data on agricultural land cover, ethnic groups distribution, terrain characteristics and the location of mineral resources, and match it with data on crop calendars as well as climate indicators like precipitation and temperature. The structure of the dataset is that of a raster grid: the cross-sectional units of observations are subnational "cells" of 1 degree of latitude x 1 degree of longitude, whose sides are placed in correspondence of integer values of latitude and longitude.

Conflict events

Data on civil conflict episodes over the period 1997-2011 are drawn from the PRIO/ Uppsala Armed Conflict Location and Event (ACLED) dataset in its Fall 2012 version. This is the most recent and detailed conflict dataset developed by PRIO/Uppsala. It codes exact location, in terms of latitude and longitude, date, and additional characteristics of a wide range of conflict-related events in states affected by civil war. Civil conflict episodes are defined broadly, to include not only battles with more than 25 casualties (the standard PRIO threshold) but all kinds of activity involving rebels, such as recruitment or the establishment of headquarters. Event data are derived from a variety of sources, mainly concentrating on reports from war zones, humanitarian agencies, and research publications. Information from local, regional, national and continental media is reviewed daily; consistent NGO reports are used to supplement media reporting in hard to access cases; and finally Africa-focused news reports are integrated to supplement daily media reporting (Raleigh et al., 2012). The result is the most comprehensive and wide-reaching source material presently used in disaggregated conflict event coding.

While this is considered a high quality dataset, and is starting to be employed in the economics literature (e.g., Michalopoulos and Papaioannou, 2012; Besley and Reynal-Querol, 2012) we must acknowledge one potential, yet unavoidable concern: selection in reporting. For instance, we cannot rule out that areas experiencing intense conflict

[7]The countries in our dataset are: Algeria, Angola, Benin, Botswana, Burkina Faso, Burundi, Central African Republic, Cameroon, Chad, Congo, Democratic Republic of the Congo, Cote d'Ivoire, Egypt, Equatorial Guinea, Eritrea, Ethiopia, Gabon, Ghana, Guinea, Guinea Bissau, Kenya, Lesotho, Liberia, Libya, Madagascar, Malawi, Mali, Mauritania, Morocco, Mozambique, Namibia, Niger, Nigeria, Rwanda, Senegal, Sierra Leone, Somalia, South Africa, Sudan, Swaziland, Tanzania, Togo, Tunisia, Uganda, Zambia, Zimbabwe.

might have a poorer media coverage, possibly leading to under-reporting of conflict. Unfortunately we have no alternative data source of comparable scope and level of disaggregation allowing us to evaluate this concern. At the same time, it is unclear that such a reporting bias would be systematically correlated with our measure of weather shocks, which is specific to the crops grown in different cells and to the growing season months of those crops.

In most of our analysis we use a broad indicator of conflict incidence, that is, a dummy equal to one if at least one conflict event of any type occurred in a given cell in a given year (*ANY EVENT*). We also consider a breakdown of conflict events into different types, i.e. battles, violence against civilians, riots and rebel recruitment, to test if our explanatory variables have a differential impact on these different outcomes.

Crop cover data

Data on the geographical distribution of agricultural crops is drawn from the M3-Crops Data by Monfreda et al. (2008), a detailed raster dataset at the 5 arc minutes x 5 arc minutes resolution (about 9.2 km by 9.2 km at the equator) including 137 crops. For each 5"x5" cell in the raster and each of the 137 crops included, Monfreda et al. report harvested area in hectares. We aggregate the harvested area variable at the lower resolution of our dataset, i.e. 1 degree x 1 degree, and we employ it to rank the crops cultivated in each cell. We identify the main crop for each cell of our dataset as the crop with the largest harvested area in the cell; we thus obtain 30 different "main crops" in our full sample.

Natural resources

In an effort to collect georeferenced data on as many natural resources as possible, data on the location of mineral resources are drawn from a combination of the Mineral Resource Data System (MRDS) prepared by the United States Geological Survey (USGS) and of the PRIO/Uppsala datasets Gemdata, Petrodata and Diadata. We have identified 85 types of mineral commodities present in the countries of our dataset, including precious metals, industrial metals, oil and gems.

PRIO natural resources datasets were compiled through an intensive literature search of academic databases and journals, national geological survey reports and industry databases and reports, and as a result they tend to be more comprehensive and reliable than USGS. However, although likely to underreport mineral occurrences, USGS data are the only comprehensive, georeferenced data source for mineral commodities available to the general public.

In the present analysis we employ a coarse indicator for the presence of any mineral in the cell. In ongoing work we are exploring the differential impact of gemstones, oil and other types of minerals, as well as the time-varying impact of these resources in

relation to changes in their prices.

Ethnic groups

Data on ethnic groups are drawn from the new University of Zurich "Geo-referencing of Ethnic Groups" (GREG) dataset. The latter relies on maps and data drawn from the classical Soviet Atlas Narodov Mira and employs geographic information systems to represent group territories as polygons. We used the maps available in the GREG data and combined them with our raster grid to measure the extent of ethnic diversity in each cell. As a proxy for ethnic grievances, we compute a cell-level Ethno-Linguistic Fractionalization (ELF) index, based on the shares of inhabited territory attributed to different ethnic groups in each cell.

Infrastructure and geography

Data on the location of roads are drawn from the Global GIS Atlas Developed by the U.S. Geological Survey, a digital atlas of the world at a nominal scale of 1:1 million. These data have no time variation and report only the roads known in year 2000. To mitigate measurement error and selection concerns, we use as a proxy for road density a dummy for the presence in the cell of at least one road of primary use.

The remaining cross-sectional geographic information are coded from the Yale G-Econ Gridded Output dataset (Nordhaus et al., 2006), from which our dataset inherits the "grid" structure and the 1 degree by 1 degree resolution.

To investigate at the disaggregated scale the relationship between mountainous terrain and conflict, we include two different measures: one is the average elevation in the cell and one is the standard deviation of elevation, denoted as "roughness"; both are measured in meters. In the conflict literature terrain ruggedness has received considerable attention, starting from Fearon and Laitin (2003); their proxy for elevation is the share of mountainous terrain over a country's surface. This is a less than perfect measure for various reasons: first, it is a measure of elevation, and not of slope: as a result, according to this measure, a plateau would count as "rugged" terrain due to its elevation, even though it does not display characteristics favorable to rebel warfare. Secondly, being expressed as a proportion of the country's territory, it is arguably measured at the wrong scale: unless the rebels indeed operate on the mountainous share of the country, the magnitude of this share should not matter. Our measure should be an improvement on both grounds.

We also include the distance from the closest navigable river - measured in km from the cell's midpoint - to capture the strategic importance of the location.

Climate data

Our main climate indicator is the Standardized Precipitation-Evapotranspiration Index (SPEI), a recently developed multiscalar drought index (Vicente-Serrano et al.,

2010). This is a departure from most of the conflict literature, which so far has focused on precipitation as the main climate indicator. One of the concerns with precipitation as such is that it might not be an accurate measure of climate shocks impacting agriculture, since the impact of rainfall on the growing cycle of a plant depends also on the extent to which water can be retained by the soil. This in turn depends on a variety of factors, including most notably temperature, but also latitude, sunshine exposure, wind speed. This information is incorporated in Potential Evapotranspiration (PET), which is defined as the amount of water that could be evaporated and transpired if there were sufficient water available. A way to take into account the different soil's ability to retain rainfall moisture is to consider a measure of precipitation corrected by PET. The Standardized Precipitation-Evapotranspiration Index (SPEI) is such an index, which considers the joint effects of precipitation and temperature. Given its multiscalar nature and its ability to incorporate the joint effects of precipitation and PET, it represents an improved alternative to more widely used indexes such as the Palmer Drought Index or Standardized Precipitation. Details on the calculation of SPEI are provided in the Appendix.

Vicente-Serrano et al. (2010) use data on temperature and precipitation from CRU TS3.0 as inputs into SPEI. However, CRU TS3.0 relies on gauge data and this has some shortcomings in the context of our analysis. The first is that given the limited number of stations present in Africa, a significant amount of interpolation needs to be done in order to produce the data at the fine level of disaggregation we are using. This interpolation may artificially generate patterns of spatial correlation in weather shocks, thus hampering our ability to estimate the "true" extent of interdependency. The second potential problem is that the availability of gauge data may itself be endogenous to conflict.

To deal with the above problems we chose to manually re-calculate the SPEI index feeding in the formula data on temperature, precipitation, and other atmospheric variables during 1979-2011 all drawn from the ECMWF ERA-Interim dataset (Dee et al., 2011).[8] The ECMWF ERA Interim archive provides re-analysis data available at a variety of grid resolutions, and with temporal resolution of up to 6 hours, for the period 1979-2011. Data are elaborated starting from high-frequency observations from a variety of sources, including weather stations, satellites and sondes. ERA Interim is considered a very high quality dataset, and represents a significant improvement over gauge data in areas with sparse weather stations like Africa.

SPEI will be our main explanatory variable of interest for what concerns climate,

[8] A previous version of the paper featured the SPEI series as originally proposed by Vicente Serrano et al. (2010). Results are available upon request.

because it encompasses all the above mentioned features of climate and of the terrain which are relevant for agricultural production. The SPEI index is expressed in units of standard deviation from the average based on the available period (1979-2011). The data is fitted to a Log-logistic distribution and normalized to a flexible multiple time scale such as 1, 4, 6, 12, 24, 48 months, etc. A short (say, 4 months) time scale reflects short- and medium-term moisture conditions and thus provides a seasonal estimation of precipitation as it is relevant for agriculture. For this reason we use SPEI at a 4 months time scale.[9]

We also consider precipitation and temperature individually, both drawn from ECMWF ERA-Interim. In particular, in order to capture the relevance of the most extreme temperature values (see e.g. Burgess et al., 2011), we construct a "temperature deviation" variable as follows. For each cell we compute the historic average over the sample 1979-2011 of the monthly daily mean temperature; then for each month we take the absolute deviation of the monthly daily mean temperature from this historic average; finally we average this monthly measure over the year.

For our exercise using future climate projections, we draw monthly projected values of precipitation and temperature during 2012-2030 under a medium emissions scenario from the CORDEX Archive, which provides gridded climate projections at a 0.44 degree resolution. In particular we use monthly total precipitation, monthly maximum and minimum daily temperatures under the CAN-ESM2 model, developed within the framework of CMIP5, under a midrange-mitigation emissions scenario (RCP4.5).

Crop calendars and crop-specific climate shocks

A key feature of our analysis is that we do not confine our measurement of climate indicators to aggregates over the year, but we try to identify periods within the year during which climatic conditions impact agricultural production the most. In particular, we construct specific indicators for climatic conditions during the growing season, which is when crops are most sensitive to unfavorable conditions. To retrieve the growing season of the main crop (ranked by harvested area) cultivated in each cell we rely on crop calendars drawn from a variety of sources.

As a primary source we use the Global Monthly Irrigated and Rainfed Crop Areas around the year 2000 (MIRCA 2000), prepared by the Physical Geography Department of the Goethe Universität Frankfurt am Main. This is a dataset of monthly growing seasons of 26 irrigated and rainfed crops at different latitudes and longitudes, with a spatial resolution of 5 arc-minutes by 5 arc-minutes. It is our preferred source given that it disaggregates by irrigated and rainfed crops - which we focus on - , and given its high spatial resolution.

[9] Our results are robust to different time scales. Results available upon request.

For the crops and cells not covered by MIRCA, we turn to two complementary sources, which both report crop calendars at the country level. The first are those generated with the FAO Food security and Early warning Network for Information eXchange Workstation (FENIX) Crop Calendar tool. The FENIX tool indicates for various crops and countries the planting and harvesting season. We define the growing season as the months comprised between planting and harvesting. Our second source are the FAO Seeds and Plant Genetic Resources Crop Calendars.

We construct measures of crop-specific climate shocks by matching our monthly climate data with the calendars of the main crops cultivated in each cell, thus creating cell-specific measures of "relevant" climatic conditions.

Our benchmark indicator of climate shock, denoted as SPEI Shock Growing Season, captures low SPEI episodes occurring during the growing season of the main crop of a given cell. It is defined at the cell-year level as follows: in a given year, consider the growing season months of the main crop; take the number of consecutive growing season months in which SPEI was below its mean by more than one standard deviation; express this measure as a fraction of the number of growing season months.[10] The value of SPEI Shock Growing Season thus ranges between 0 and 1, with 0 denoting a "good" year in which never during the growing season of the main crop SPEI assumed abnormally low values, and 1 denoting a "bad" year in which the entire growing season witnessed abnormally low values of SPEI.

For different climate indicators - rainfall and temperature absolute deviation - we also define "Growing Season-adjusted indicators" constructed as follows: we compute monthly interactions between a growing season dummy and the monthly climate indicator, and we average these monthly interactions over the year. This amounts to computing a weighted average of monthly rainfall or temperature absolute deviation assigning a weight 0 to months outside the growing season of the main crop.

3.2 Descriptive statistics

Descriptive statistics are reported in Table 1. Panel A reports statistics at the cell level for the cross-sectional estimates we will perform in Table 2; Panel B instead reports statistics at the cell/year level for the balanced panel used in the rest of the analysis.

[Insert Table 1]

[10] In case there are more than one consecutive spell of low SPEI during the growing season in a given year, we consider the longest spell. Our results are robust to considering instead the first spell in the year. Note that SPEI is already expressed as standard deviations form the cell's historic mean over the whole available period 1979-2011. For the purpose of defining our variable, we re-normalize it based on the mean over our sample period, which is slightly lower than the historic mean.

Cell level incidence of conflict is very high: the average cell in our sample has experienced conflict episodes for 17% of the years in our full panel, which means 2.5 years. The territory in our sample appears to be mineral rich, as 21% of the cells have at least one mineral deposit, and on average moderately elevated, with an average elevation of 315 meters. Ethnic fractionalization also appears to be high, with an average cell-level ELF index of 20%. We include among our cross-sectional controls a "shared" dummy for cells which do not belong entirely to one country, but contain a country border; these cells are about 25% of our sample. The dummy "border", on the other hand, identifies cells whose edge coincides with a state border (about 5% of our sample).

[Insert Figures 1 to 5]

In Figures 1-5 we map some of our key variables, to have a sense of the within-country variation in our covariates. Figure 1 shows cell-level conflict prevalence, reporting the fraction of years during 1997-2011 in which the cell experienced at least one conflict event. Conflict appears to be clustered in space, and in particular the conflict clusters in the Great Lakes region and in West Africa are very apparent. Overall, areas in the tropical belt appear to have experienced more conflict, which could induce a positive spurious correlation between rainfall levels and conflict incidence. Our climate shock indicator, which considers deviations from the cell historical mean, helps address this problem.

Figure 2 plots average rainfall levels, which as expected are higher at the tropics and display a strong spatial correlation. Figure 3 plots the average SPEI index. Although it also appears to be spatially clustered, it displays much more local variation than rainfall, suggesting it might be a better explanatory variable. The plot substantiates the claim that SPEI incorporates distinct information from rainfall. Figure 4 shows the historic mean of the absolute temperature deviation. Again, considerable within-country variability appears in temperature deviations from the cells' historical mean.[11]

Finally, in Figure 5 each cell is associated with a color corresponding to the main crop cultivated in the cell. The map shows that a wide range of crops are cultivated in our sample, and there is considerable variation in their spatial distribution. This suggests that focusing on the growing season of one crop "representative" of the whole Sub-Saharan African continent would provide a very limited picture of the true cultivation pattern. Indeed we can derive significant variation across cells and across months in climate measures thanks to variation in the growing seasons of different crops.

[11] In the Appendix we report, for comparison, figures 2, 3, and 4 constructed considering climate indicators in a given year (2000) rather than their sample average.

4 Empirical results: cross section

In this section we explore the empirical determinants of civil conflict starting with time invariant characteristics such as geography and location of mineral deposits. Our interest in conducting this type of analysis hinges on two factors. First, despite the limitations of cross-sectional inference, the high level of spatial resolution of our data limits the concerns related to state-wide unobservable determinants of conflict and allow us to pin down the relationship between each factor and the location in which conflict occurs with more confidence. Second, the data exhibits spatial dependence, in the sense that geographic features in a given cell may affect not only the cell itself but also neighboring cells. This is something that we can test and that potentially yields interesting insights on the interdependence among neighboring locations in the diffusion of conflict.

[Insert Table 2]

Our cross-sectional evidence is presented in Table 2. The table reports OLS coefficients and standard errors in parentheses corrected for spatial dependence following Conley (1999). The dependent variable captures average conflict incidence and is the fraction of years during the sample period in which the cell has experienced at least one conflict event. The mean and standard deviation of this variable are, respectively, .17 and .25.

In columns 1 and 2 we consider "own" characteristics of the cell (Model I), in columns 3 and 4 we also include characteristics of the neighboring cells (Model II) and in columns 5 and 6 (Model III) we estimate a spatial lag model in which we further include a spatially autoregressive component to capture direct conflict spillovers across neighbors. Neighbors are defined according to our benchmark weight matrix as cells whose midpoints lie within 180 km from the midpoint of the own cell. Columns 1, 3 and 5 report the coefficients of a purely cross-sectional regression without area fixed effects. In columns 2, 4 and 6 we instead include country fixed effects (and their spatial lags, for columns 4 and 6). The specifications that include country fixed effects are our preferred ones because our focus is on within-country variation in the incidence of conflict, and by including country fixed effects we account for time-invariant aspects of the political, economic or social structure of the states in our sample, as well as for state-level geographic features, e.g. country size.

Let us consider first own characteristics of the cell. The first set of controls we include measure geo-administrative characteristics: *Shared* is a dummy for whether a cell belongs to more than one country, and *Border* is a dummy for whether a cell's side is tangent to a country border (the two are mutually exclusive). The idea is that cells which are at the

border with other countries may be more likely to experience conflict. The coefficient for *Shared* is positive and significant in all specifications, consistent with this hypothesis. The *Border* coefficient, on the other hand, is statistically indistinguishable from 0. The third control listed in the table, *Area*, measures the area of the cell corresponding to land, to account for coastal cells which correspond mostly to sea. The coefficient of this variable is virtually zero in all specifications. We next move to geographic characteristics of the terrain. The first, *Elevation*, measures the average altitude of the cell (in mt.). Its coefficient is always negative and significant, indicating that locations at higher altitudes are on average less prone to conflict. Our second proxy for geography, the variable *Rough*, is the standard deviation of elevation in the cell, and thus captures the roughness of the terrain. This variable is strongly and significantly correlated with conflict incidence. A one-standard deviation increase in roughness increases conflict incidence by .043 in column 6 - our preferred specification, that is one fourth of the mean of the dependent variable. This confirms a relationship which has been previously highlighted in cross country studies, starting with Fearon and Laitin (2003), and which is usually attributed to the fact that impervious areas provide safe havens for rebels.

We next consider the variable *Distance to river*. This is the minimum distance (in km) of the centroid of the cell from a navigable river. The negative coefficient of this variable in columns 1-2 and 5-6 suggests that areas further away from navigable rivers tend to experience less conflict. This could depend on the fact that these areas are more controlled by local governments or simply less prosperous in the long run, so that they are less appealing for predation purposes. This is also consistent with findings by Gleditsch et al. (2006), who note that the presence of a shared river basin is associated to higher conflict risk.

Transport infrastructure plays a significant role, as confirmed by the coefficient of the variable *Road*, which is a dummy equal to one if the cell contains at least one road of "primary use" (as defined by the Global GIS Atlas). The coefficient of this variable is around .10 across the various specifications, remaining highly significant in all cases. The magnitude of the effect suggests that the presence of a road in the cell increases the fraction of years with conflict by .4 standard deviations. One possible interpretation is that areas served by main roads are easier to reach for the purpose of attacks. Another interpretation is again that the long terms benefits of capturing those areas are higher compared to areas not covered by main roads.

We next turn to some of the channels more widely explored in the cross country literature. The first is linked to the literature on ethnic fractionalization. We compute an equivalent of the ELF index in which we use, rather than population shares of different ethnic groups, the relative territory shares occupied by each group as reported by the GREG dataset, after having normalized these shares by the total inhabited land in

each cell. This is a proxy for the degree of ethnic diversity in the cell, which may be associated with "grievance" motives for conflict. The average cell in our sample has 2 ethnic groups, with an *ELF* of 0.2. The coefficient of this variable is positive and significant in virtually all regressions, with a magnitude ranging from .04 to .08. This implies that a one standard deviation increase in *ELF* on average is associated with a 1 to 2 percentage points higher fraction of years with conflict, a 5 to 10 percent effect.

The second channel is linked to the natural resource curse. The variable *Minerals* is a dummy equal to one if the cell contains at least one mineral deposit (21 percent of the cells in our sample have at least one such deposit). Ceteris paribus, the presence of minerals in the cell is associated with a significantly higher incidence of conflict, in the order of about one fourth of a standard deviation of the dependent variable. This coefficient is very stable in terms of size and significance across specifications. The effect of this variable can be explained in two (non-mutually exclusive) ways. On the one hand, there can be "greed" motives, as competing forces may try to capture territory that promises high revenue from mineral extraction. On the other hand, control over mineral resources yields a flow of cash revenue that rebels and government can use to finance their military activities.[12]

Let us now turn to neighbors' characteristics, represented by the spatial lags of the covariates considered above. Most neighbors' characteristics are statistically insignificant, suggesting, in general, that the impact of the geographic characteristics discussed above is a strictly local one. Having a neighbor that is bordering another state is associated with more conflict in columns 5 and 6, possibly due to separatist conflicts.

Finally, let us consider conflict spillovers. The autoregressive term in columns 5 and 6 appears highly significant and goes from .047 when we do not include country fixed effects to .024 when we do. Based on the latter (more conservative) estimate, a cell that had one of its neighbors experiencing conflict for the entire sample period experiences conflict for 2.4 percent more of the years, which is 1/10 of a standard deviation. Considering that the average number of neighboring cells in our sample is 7.4, a cell surrounded by neighbors all of which had conflict throughout the period would be in conflict 18 percent more of the time, that is .7 of a standard deviation, and would imply doubling the fraction of years in conflict compared to the mean. Note that, however, this analysis employs a definition of conflict prevalence with no time variation: this should only be taken as suggestive evidence that conflict spillovers in space are relevant, as only the

[12] According to the theoretical literature there is a third, indirect channel through which mineral wealth can fuel conflict, i.e., by increasing rent-seeking and corruption phenomena, which weaken states and their ability to effectively govern and maintain security. This third effect, though, is not captured at the scale of our study, as it is mediated through a country's institutions (which in our study are partly controlled for by the inclusion of country dummies).

panel analysis can provide adequate estimates of both temporal and spatial spillovers.

Overall, our cross-sectional analysis suggests that geographic characteristics have a strictly local effect, especially terrain ruggedness and presence of mineral endowments, and that cross-cells conflict spillovers are potentially very relevant.

5 Empirical results: panel

We next turn to the analysis of climatic factors as determinants of conflict. For this purpose we exploit the rich temporal dimension of the data and conduct the analysis at the cell/year level. Our dependent variable becomes $ANY\ EVENT_{\mathrm{t}}$, a dummy equal to one if the cell experienced at least one conflict event during year t. We consider three models: a non-spatial, static model (Model I), in which we include climate shocks in the own cell only; a non-autoregressive, spatial static model (Model II), in which we consider climate shocks both in the own and neighboring cells; and a fully spatial, dynamic Durbin model (Model III) in which we also include two autoregressive terms: a spatial lag of the dependent variable, to capture contemporaneous conflict spillovers over space, and a temporal lag, capturing temporal conflict persistence in the own cell. The first two models are estimated by OLS, with standard errors corrected for spatial and temporal correlation, while the third model is estimated by MLE. All regressions include country and year fixed effects, plus the controls listed in Table 2; Models II and III include the spatial lags of controls and country fixed effects; these coefficients are not reported for ease of exposition.

We will first present our benchmark specification, in which we highlight the relationship between cell-specific weather shocks and conflict, accounting for spatial dependence. We then consider two important issues arising in spatial econometrics: the choice of the weighting matrix and the choice of scale. We then turn to alternative climate indicators, and finally we attempt an analysis disaggregated by type of conflict event.

5.1 Benchmark estimates

[Insert Table 3]

Table 3 contains our main results. The regressor of interest is *SPEI Shock Growing Season*, defined as the fraction of the main crop's growing season during which SPEI was below its cell-level mean by one standard deviation or more. As explained in Section 4, the SPEI index considers the joint effects of precipitation, potential evapotranspiration and temperature, higher values of this index corresponding to higher levels of "effective"

rainfall. In our specifications we also control for standalone SPEI, which in this specification captures the impact of SPEI in months outside the growing season of the main crop. The first and second temporal lag are included for all climate indicators.

In column 1 *SPEI Shock Growing Season* displays a strong, highly significant correlation with conflict, both contemporaneous and in its two temporal lags, indicating that spells of low SPEI during the growing season are associated with more conflict. The impact of the standalone SPEI variable is not significantly different from zero, with the exception of the first lag which is marginally significant at the 10 percent level (but this does not survive the inclusion of spatial and temporal lags of the endogenous variable in column 3). This is consistent with the idea that climatic conditions during the growing season are those which matter the most for agriculture. The specification in column 1, however, fails to take into account spatial and temporal correlation; this could create omitted variable bias.

We then turn to Model II (column 2), which addresses the issue of spatial correlation in the covariates by including spatial lags of all the independent variables. In this specification, the contemporaneous *SPEI Shock Growing Season* remains positive but loses statistical significance, while the first and second lags are unaffected both in size and in significance. The fact that conflict responds with a one and two year lag is consistent with the kind of temporal persistence highlighted in cross country studies (e.g., Ciccone, 2011). Interestingly, shocks to neighboring cells have a precisely estimated zero effect on own cell conflict, pointing to a strictly local direct effect of weather shocks.

Although Model II controls for climatic conditions in the surrounding cells, it may still suffer omitted variable bias from not including autoregressive components of the dependent variable. We address this issue in column 3 (Model III). First note that including autoregressive components tends to reduce the magnitude of the coefficients estimated in Model II, but only to a minor extent: the coefficients of the first and second lag of *SPEI Shock Growing Season* in the own cell go from $-.05$ to $-.04$ and retain significance at the 5 percent level. A spell of SPEI below one standard deviation throughout the whole growing season is associated to a 4 percentage point increase in conflict likelihood in the subsequent year, and a further 4 percentage point increase in the year following that; this is roughly one fourth of the mean of the dependent variable each year. The combined direct effect of a shock over three years is .09, that is over half of the mean. The effects are thus quite sizeable.

Conflict spillovers, both in time and space, appear to be very significant. Conflict in the own cell is associated to a 33 percentage point increase in the probability of experiencing conflict the following year. Contemporaneous conflict in one of the neighboring cells induces a 4.5 percentage point increase in the probability of experiencing conflict in the cell itself. Given that according to our definition of contiguity matrix the average

cell in our sample has 7.4 neighbors, this means that conflict in all of the neighbors induces a 33 percentage point increase in the probability of conflict in the average cell itself. Overall it seems that temporal persistence within cells is more relevant than contemporaneous spatial spillovers across cells, although the spatial spillovers are sizeable and significant.

In Section 5.6 we discuss how the total impact of climate shocks, including the feedback effects through conflict in neighboring cells, can be quantified. In the next section we explore the sensitivity of our estimates to different choices of spatial weighting matrix.

5.2 Sensitivity to distance and spatial resolution

[Insert Table 4]

Just as in time series the structure of temporal dependence is assumed by the researcher and is not estimated, so is the structure of spatial dependence - encompassed by the spatial weighting matrix - in spatial econometrics. The most popular choices for spatial weighting matrix are binary contiguity matrices, like the one we employ in our benchmark, or matrices based on the inverse geographic distance, linear or squared. In our case binary matrices seem the most appropriate given the structure of the grid, as we do not have a continuous measure of distance from the centroid of the cell but rather a step-wise distance function that changes when we move from one cell to the next. In Table 4 we thus re-estimate the specification of column 3 in table 3 using different binary contiguity matrices.

Column 1 reports our benchmark estimates for the sake of comparison. In columns 2, to 4 we estimate our model using binary contiguity matrices with different distance cutoffs: 290, 450 and 600 km. A 290 km distance cutoff implies that we are potentially considering as a cell's neighbors not only the 8 adjacent cells but also the next immediate circle of adjacent cells, and increasing it further to 450 we add yet another circle. Finally, with a cutoff of 600 km, we are considering a large, approximately circular area around the reference cell. With distance cutoffs of 290, 450 and 600 km the average number of neighbors for each cell is respectively 18, 44 and 81.

When we increase the radius of our distance matrix the coefficient on the first temporal lag of *SPEI Growing Season Main Crop* becomes increasingly smaller and loses significance; on the other hand the coefficient on the second lag appears remarkably stable in size and significance. The temporal autoregressive coefficient is also very stable around the value of .33, and significant at the 1 percent level in all specifications.

On the other hand, as expected, the choice of weighting matrix does affect the coefficients of the spatially lagged variables. In particular, the spatial autoregressive coefficient (the coefficient on $W \cdot X$) is most significantly affected by changes in the definition of neighborhood, decreasing in magnitude as we increase the distance cutoff. This reveals that as we broaden the definition of neighbors, the contribution of each individual neighbor becomes smaller, which is intuitive: as we add neighbors further away from the cell, and presumably with a smaller absolute impact on conflict in the reference cell, the impact of the average neighbor is driven down.

Overall this analysis seems to suggest that own effects are quite stable as we change the definition of weighting matrix. Since our focus is on the local dimensions of conflict, we choose as our benchmark matrix one with a relatively restrictive definition of neighbors, i.e. the 180 km radius which corresponds to the adjacent cells.

Another critical specification issue arising when dealing with spatial data is the so-called Modifiable Areal Unit Problem (MAUP), a well-know phenomenon in spatial analysis. It is defined as "a problem arising from the imposition of artificial units of spatial reporting on continuous geographical phenomenon resulting in the generation of artificial spatial patterns" (Heywood et al., 1998). The MAUP consists of two components: one is a scale problem, which is the variation in numerical results occurring due to number of zones used in analysis, and hence the possibility of obtaining different results for different resolutions; the other is an aggregation problem or zonation effect, which refers to which zoning scheme is used at a given level of aggregation. Although not eliminable, this problem is mitigated when the units of observation are equal-sized cells rather than administrative units of different sizes: at that point, the zonation effect will be minimal, even though a scale effect nevertheless exists. Despite the lack of general solutions, a simple strategy to deal with the problem, is to undertake the analysis at multiple scales or zones. In Table 5 we repeat our analysis for larger scales of aggregation: 2 by 2 and 3 by 3 degrees cells.

[Insert Table 5]

First we construct "macro-cells" of 2 by 2 degrees composed by aggregating 4 of our 1 by 1 original cells. This new, lower-resolution grid can be constructed in 4 different ways depending on where the "macro-cells" are centered. We run our benchmark Table 3 specification in each of these four possible grids. We use a binary contiguity matrix with a 390 km cutoff, so that each macro-cell's neighborhood is formed by the 8 adjacent macro-cells. In Panel A of Table 5 we report the average coefficients and average standard errors obtained from running our Model I and Model III benchmark in the four different grids. We also report the standard deviation of each estimated coefficient across the four

grids, to have a sense of how sensitive the results are to the centering of the macro-cells. We repeat this kind of analysis for an even lower resolution, by constructing a panel of 3 by 3 degrees cells. In this case the new grid can be centered in 9 possible ways. Panel B of Table 5 reports the results of the analysis in those 9 panels. The binary contiguity matrix in this case has a cutoff of 490 km, so that each macro-cell's neighborhood is formed by the 8 adjacent macro-cells.

The analysis highlights the following patters. First, the centering of the grid does not seem to affect the results in a very significant way, as shown by the low standard deviation of the estimated coefficients across grids. This indicates that the zonation effect is limited when using the "grid" approach. This is an important robustness check which we can conduct at these lower resolutions and not with our original 1 by 1 cells - in that case the grid cannot be re-centered due to constraints in data availability. Secondly, changing the resolution does not affect the sign of the relevant parameter estimates, but affects the magnitude: the coefficients of own cell covariates appear to increase in magnitude as the resolution decreases. This effect is documented in the MAUP literature (Fotheringham and Wong, 1991): the correlation coefficient for variables of absolute measurement typically increases when areal units are aggregated contiguously. The reason is that the aggregation process involves a smoothing effect, by averaging the relevant variables, so that the variation of a variable tends to decrease as aggregation increases. When the variances of X and Y variables decrease, the correlation coefficient will increase if the covariance between X and Y is relatively stable. Finally, the statistical significance of the relevant covariates tends to decrease at intermediate resolutions - this is especially apparent in Model III estimates. This possibly reflects a trade-off between estimating the "true" model (which we hypothesize is at higher resolution) and the fact that aggregation implies smoothing, hence less noise.

5.3 Other climate indicators

We next turn to other potential climate indicators that have been employed in the cross country literature. The first is a crude measure of rainfall, measured in logs of yearly values (in millimeters), and the second is Temperature Absolute Deviation, which is the absolute deviation of the temperature from the historical mean for the cell. For each of these two climate indicators, we compute a "Growing Season Indicator" obtained by averaging the monthly values of the variable only over the growing season of the main crop. Table 6 reports Model I, II and III specifications in which we include both the standalone climate measure and the corresponding growing season indicator for rainfall (cols. 1 to 3) and temperature (cols. 4 to 6).

[Insert Table 6]

In columns 1 to 3 the coefficients on rainfall are typically insignificant, which runs against the findings in the cross country literature. While apparently surprising, this result is easily understood when considering the patterns of rainfall in Figure 2 and conflict in Figure 1. Average rainfall is in fact high at the tropics and exhibits relatively less within country variation compared to SPEI (see, e.g. Figure 3). This generates a positive correlation between rainfall and conflict that may counterbalance the negative relationship implied by some of the theories. Furthermore, simply measuring rainfall fails to take into account differences in temperature, soil, and other conditions that may be crucial in terms of effects of climate on agricultural production.

Turning to temperature, there is some evidence from columns 1 and 2 that (lags of) temperature shocks during the growing season increase the likelihood of conflict, consistent with Burke et al. (2009). However this effect appears non-significant once we account for intertemporal persistence and spillovers in Model III (col. 6).

The above results seem to suggest that neither rainfall alone nor temperature alone adequately capture the local level relationship between conflict and climate. For this reason we prefer the SPEI index, which captures the combined effects of precipitation and potential evapotranspiration, which in turn depends on temperature as well as latitude, month of the year, number of sun hours, etc.

In Appendix Table A1 we show two alternative SPEI-based indicators: standalone SPEI and a continuous measure of SPEI during the growing season. In column 1 standalone SPEI has the expected negative sign, but it is no longer a significant conflict predictor once spatial lags are included (columns 2 and 3), suggesting that indeed what matters are climatic conditions during the relevant growing season. In columns 4, 5 and 6 we show an alternative indicator of SPEI over the growing season, computed by averaging monthly SPEI over growing season months for the main crop. Unlike our benchmark indicator, this measure is not confined to severe SPEI negative shocks. Our estimation results indicate that low SPEI over the growing season is associated with more conflict, but the predictive power of this indicator is inferior to our benchmark one (only the first lag is statistically significant).

5.4 Different types of conflict events

We now turn to a disaggregation of conflict events into four different types, based on the ACLED classification. The dummy $BATTLE$ is equal to 1 when a cell/year has experienced a battle of any kind, either one where control of the contested location does not change, or one where the government or the rebels take control of a location

previously occupied by the other contestant. The dummy *CIVILIAN* captures violence against civilians, defined in ACLED as instances where "any armed group attacks unarmed civilians within a larger conflict". This is the type of event most closely related to possible predation motives. A third type of event is riots and protests (dummy *RIOT*), i.e. instances in which "a group is involved in a public meeting against a government institution." Finally, ACLED also codes rebel activities such as the establishment of a base or headquarter (which can be non-violent) as well as recruitment drives and incursions (dummy *REBEL*). This is the variable where we should expect to find effects according to theories that stress rebel recruitment and the opportunity cost of fighting as an underlying rationale for the link between rainfall shocks and conflict. Summary statistics for these dependent variables, reported in Table 1, indicate that the average frequency of these events in the cell/years in our sample is .10 for battles, .10 for violence against civilians, .06 for riots and .03 for rebel recruitment. The last class of events is thus relatively rare, which limits the power of the specifications we estimate in this section, yielding relatively noisier estimates.

[Insert Table 7]

In Table 7 we estimate a series of cross-sectional regressions (Models I, II and III) along the lines of what we did in Table 2, but the dependent variable is now disaggregated according to the type of conflict event: battles in columns 1-3, violence against civilians in columns 4-6, riots in columns 7-9 and rebel recruitment in columns 10-12. The following patterns can be detected.

First, the coefficient of spatial autoregressive term (Model III) is positive and highly significant for all dependent variables except riots, suggesting that spatial spillovers exist for most types of events. Second, characteristics such as rough terrain, the presence of roads and mineral endowments positively correlate with all types of events. Third, other characteristics impact differentially the different types of events. One example is the variable *Shared*, which identifies cells that contain a country border. This variable has a positive and significant impact on rebel recruitment, on the occurrence of battles (likely for the control of territory) and on violence against civilians, but no impact on riots.

[Insert Table 8]

We next turn to the effect of climate shocks on different conflict events using panel data. In Table 8 the coefficients of the autoregressive terms, both in space and time, appear to be remarkably similar for battles, violence against civilians and rebel recruitment.

The coefficients in the riots regression display relatively more persistence in time than in space, suggesting that violent episodes are more likely to spill over in space compared to non-violent ones. The coefficients on own climate shocks point in the same direction as the results we obtained for the aggregate dependent variable, i.e. years with long spells of low SPEI during the growing season are associated with more battles, more violence against civilians and more riots. The estimates are not significant for rebel recruitment (columns 10-12). This is to some extent surprising if one considers prominent theories based on the low opportunity cost of rebel recruitment during economic downturns. At the same time this dependent variable may be particularly prone to measurement error, e.g. because recruitment activities more easily go undetected compared to battles or violent events – and indeed according to ACLED rebel recruitment only occurs in 3 percent of the cell/years in our sample.

5.5 Impact magnitude and projections

One of the features of our benchmark specification (Model III) is that a one-time shock propagates in time and space feeding back into the process through autoregressive terms. For this reason, the impact of a covariate X in a given cell on the dependent variable Y in that same cell is not entirely captured by the parameter estimates from equation (3). For instance, the coefficient 0.04 from Table 3 should be interpreted as the direct impact of a SPEI growing season shock on next period's conflict incidence in the own cell. However, a shock in the own cell affects also conflict in neighboring cells, which in turn affect contemporaneous conflict in the own cell through the spatial lag term. As a result, current conflict in the own cell is amplified. Moreover, the effects of a one-time shock to our main explanatory variable will persist in time, due both to the temporal autoregressive term in time and to the fact that two lags of the explanatory variables are included in the specification. Finally, all these impacts will propagate in space, due to the spatial lag terms. With such a specification it is therefore not immediate to see what the total effects of a one time shock can be both in the own cell as well as the neighboring cells.

In order to get a more precise quantitative assessment of the overall impact of the shock on conflict we conduct an exercise similar in spirit to the evaluation of an impulse response: we consider Model III and start with a setting in which all explanatory variables and prior conflict are set to 0; we then provide a hypothetical cell with a one-time *SPEI Shock Growing Season* equal to 1 - corresponding to a year with an entire growing season affected by drought -, while leaving to 0 all other covariates both in the own and the neighboring cells; finally, we use the coefficients estimated in Table 3 to track the estimated marginal impact of this one-time shock on the dependent variable in subse-

quent periods, leaving all other covariates to 0, in the own as well as the neighboring cells. In Figures 6 and 7 we report the results of this exercise.

[Insert Figures 6 and 7]

Figure 6 plots the marginal impacts of the one-time increase in *SPEI Shock Growing Season* on conflict incidence in the 9 subsequent periods, in a hypothetical cell as well as in its average neighbor, according to the 180 km cutoff definition. The blue line represents the dynamic response of the own cell, whereas the red line represents the dynamic response of an average neighboring cell. At $t = 1$ the one-time shock occurs in the own cell. Conflict in the own cell increases due to the direct effect of coefficient β_{21} of equation (3), but this is amplified by the fact that neighbors are affected by the current shock: their conflict increases too - as can be seen from the neighbor's impulse response - and this feeds back into the conflict of the own cell. These feedback effects, however, seem to be small: the total contemporaneous marginal impact is very close to the 0.01 coefficient estimated in Table 3. In the second and third period, although no additional shocks occur, conflict in the own cell still increases - indeed, the largest marginal increase occurs in the third period. At time 3 the total marginal impact is 0.06, 2 percentage points higher than the estimated coefficient of the variable *SPEI Shock Growing Season*$_{t-2}$in Table 3. This amplification results both from the the autoregressive term in time and from the indirect feedback effects through the neighbors. After period 3 the marginal effects start fading away. As expected, the effect of a SPEI shock on neighboring cells is small: neighbors are affected by the shock only through the spatial lags of *SPEI Shock Growing Season*- whose estimated coefficients are however close to 0 - and, more importantly, through the spatially autoregressive term. The response of neighbors roughly mirrors that of the own cell at a much smaller scale. However,it appears to be more persistent in time. The reason is that neighbors are adjacent to the own, high-conflict cell, which feeds in their own conflict at each period.

Figure 7 reports the results of the same exercise, but focusing on space instead of time. For time periods 1, 4, 7 and 10 we map on a grid of cells the different marginal impacts of the one-time shock on different cells, depicting larger impacts with darker shades. The cell which receives the one-time shock is at the center of the grid and is marked by an x. In period 1 the own cell experiences the largest increase in conflict incidence, but the neighboring cells are affected as well, although to a smaller extent. The definition of neighbors allows only the 8 adjacent cells to be directly affected by cell x through their spatial lag terms. However, conflict induced by the one-time shock to cell x does propagate also to cells beyond those immediately adjacent, due to spillovers from the immediately adjacent cells. Figure 7 shows how this propagation mechanism

resembles that of a concentric wave: the closer a cell is to cell x, the sooner the cell is contaminated, and the sooner the effect will start fading away.

The exercise above illustrates how a one-time, artificial shock of magnitude 1 affects our dependent variable of interest over time. The same method can be used to feed in the process *actual* shocks, which naturally occur at repeated time periods and locations, and need not be of size 1. We apply this method to forecast marginal conflict changes induced by projected *future* shocks in SPEI. We repeat the procedure outlined above feeding into the process forecasted values of *SPEI Shock Growing Season*, based on cell-level climate projections for 2012-2030 from the CORDEX Archive. This allows us to have a sense of how climate change will affect conflict likelihood, all else being equal and under the assumption that the responsiveness of conflict to SPEI shocks remains constant in the future.

The first step in this exercise entails predicting future SPEI shocks. Given that SPEI is by construction a standardized measure, with mean 0 and standard deviation 1 in the reference sample, simply recalculating the SPEI index with projected climate data would yield an index which is not comparable with the one used in our 1997-2011 analysis. However, we can still use climate projections to construct an equivalent of our *SPEI Shock Growing Season* measure for years 2012-2030. We do so by exploiting the mapping between SPEI (which is standardized) and climatic water balance - the input of SPEI, which is defined in absolute terms as precipitation minus PET (see the Appendix for details). Recall that our *SPEI Shock Growing Season* variable is based on whether a cell in a given growing season month experienced a level of SPEI less than one standard deviation below its average 1997-2011. The threshold is the same for all cells in terms of SPEI (i.e., one standard deviation), but this corresponds to different, cell-specific *thresholds* in terms of *water balance* (say, threshold $\overline{w}_c$ for each cell). Using projections for future precipitation and temperature under a medium emission scenario, we compute future projected water balance. In the 2012-2030 sample we then define a SPEI shock as occurring in months when projected water balance falls below the absolute threshold $\overline{w}_c$ estimated above. This is then aggregated over growing season months to construct a measure equivalent to the one used in our 1997-2011 analyses.

[Insert Figures 8 and 9]

We find that, other things equal, shocks to SPEI occurring during the growing season, as per definition of our main explanatory variable, should become more than twice as frequent during the next 20 years. The average of *SPEI Shock Growing Season* - which is 0.10 in our 1997-2011 sample - becomes 0.25 in the 2012-2030 projected sample. Average projected values of *SPEI Shock Growing Season* 2012-2030 are reported in Figure 8.

From our exercise we obtain for each cell and year the marginal change in conflict incidence induced by SPEI growing season shocks. At a given point in time this marginal change will reflect both current and past shocks, both among neighbors and in the own cell, due to the mechanisms we have discussed when commenting Figures 6 and 7. In Figure 9 we show these marginal changes in each cell, averaged over 2012-2030. The shade in each cell represents the marginal increase in conflict resulting from SPEI Growing Season shocks, in an average year 2012-2030. The pattern clearly overlaps with that in Figure 8, but there appears to be more smoothing over space - this is expected and results from the propagation mechanism described above. The estimated magnitudes are sizeable: in an average year, conflict increases by 7 percentage points due to SPEI shocks, with peaks in some cells above 20 percentage points. These large magnitudes are found in cells which have a history of repeated SPEI shocks over the years. Overall this suggests that future climate condition should have significant effects on local conflict incidence, all else being equal.

6 Conclusions

In this paper we conduct a spatially disaggregated analysis of the empirical determinants of conflict in Africa over the period 1997-2011. We exploit within-year variation in the timing of weather shocks and in the growing season of different crops, as well as spatial variation in crop cover, to construct an original measure of shocks that are relevant for agricultural production. We find that negative weather shocks which occur during the growing season of the main crops cultivated in the cell have a sizeable effect on conflict incidence. We also use state of the art spatial econometric techniques to test for the presence of temporal and spatial spillovers in conflict, and we find both to be sizeable and highly statistically significant. These results indicate that caution should be exerted when interpreting results of studies which do not incorporate spatial dynamics at all. Finally, we use our estimates to predict potential future conflict scenarios induced by climate change, under the assumption that the responsiveness of conflict to weather shocks remains constant in the next two decades. We predict that under a midrange emissions scenario severe shocks occurring during the growing season, as per definition of our main explanatory variable, should become 2.5 times as frequent during the next two decades. This in turn leads to an increase in average conflict incidence of 7 percentage points, according to our benchmark estimates.

Our findings indicate that conflict risk does not affect all the territory of a state in the same way: the correlates of civil conflict have a strong local dimension, and the likelihood of conflict likelihood is not constant in time nor in space, even within the

same country. This seems to suggest that policy interventions, be them in the form of monitoring, prevention or peacekeeping efforts, could be and should be targeted both in space and time. Our findings may be especially relevant when assessing appropriate policy responses to global warming scenarios. Given the link we trace between shocks affecting agricultural yields and conflict risk, policies aimed at mitigating the effects of climate change on African agriculture may be particularly desirable. These include the development of drought resistant crop varieties, as well as investment in irrigation and schemes to improve soil water retention. On the other hand, complementary measures to reduce the adverse impacts on incomes, such as weather-indexed crop insurance, also constitute a valuable policy option.

Finally, given the increasing availability of high resolution data (e.g., gridded datasets) and the growing number of research contributions that employ this data to address important development questions, our study can hopefully provide a number of insights and methodological indications that are useful for future work.

References

[1] Alesina, A., P. Giuliano, and N. Nunn (2011), "On the Origins of Gender Roles: Women and the Plough", NBER Working Paper 17098.

[2] Anselin, L. (1988), *Spatial Econometrics: Methods and Models*, Boston, Kluwer, Academic.

[3] Besley, T. J., and T. Persson (2008),"The Incidence of Civil War: Theory and Evidence", NBER Working Paper 14585

[4] Besley, T. J., and M. Reynal Querol (2012), "The Legacy of Historical Conflicts. Evidence from Africa", mimeo, London School of Economics and Universitat Pompeu Fabra.

[5] Blattman, C. and Miguel, E. (2010), "Civil War", *Journal of Economic Literature*, 48(1), 3–57.

[6] Brückner, M. and A. Ciccone (2011), "Rain and the Democratic Window of Opportunity", *Econometrica,* 79(3), 923-47.

[7] Buhaug, H. (2010), "Climate Not to Blame for African Civil Wars.", *Proceedings of the National Academy of Sciences of the USA* 107 (38): 16477–16482.

[8] Buhaug, H. and Gleditsch, K. S. (2008), "Contagion or Confusion? Why Conflicts Cluster in Space", *International Studies Quarterly* 52(2), pp. 215–233.

[9] Burgess, R., O. Deschenes, D. Donaldson and M. Greenstone (2011), "Weather and Death in India", mimeo.

[10] Burke M. B., E. Miguel, S.Satyanath, JA. Dykema JA, and D.B. Lobell (2009). "Warming Increases the Risk of Civil War in Africa", *Proceedings of the National Academy of Sciences of the USA* 106(37): 20670–20674.

[11] Chassang, S. and G. Padro-i-Miquel (2009), "Economic Shocks and Civil War", *Quarterly Journal of Political Science* 4(3): 211-228.

[12] Ciccone, A. (2011), "Estimating the Effect of Transitory Economic Shocks on Civil Conflict ", mimeo.

[13] Collier, P., and A. Hoeffler (1998), "On the Economic Causes of Civil War", *Oxford Economic Papers*, 50, 563-573, 1998.

[14] Conley, T. G., (1999), "GMM estimation with cross-sectional dependence", *Journal of Econometrics* 92(1), pp. 1-45.

[15] Dal Bó, E. and P. Dal Bó (2011), "Workers, Warriors, and Criminals: Social Conflict in General Equilibrium", *Journal of the European Economic Association*, 9(4), 646-77.

[16] Dee, D.P. et al. (2011), "The ERA-Interim reanalysis: configuration and performance of the data assimilation system", *Quarterly Journal of the Royal Meteorological Society*, 137 (656), 553–597.

[17] Dell, M. (2012), "Insurgency and Long-Run Development: Lessons from the Mexican Revolution", mimeo.

[18] Dell, M., B.F. Jones and B.A. Olken (2012), "Temperature Shocks and Economic Growth: Evidence from the Last Half Century", *American Economic Journal: Macroeconomics* 4 (3), pp. 66-95, July 2012.

[19] Dube, O. and J. Vargas (forthcoming), "Commodity Price Shocks and Civil Conflict: Evidence from Colombia," *Review of Economics Studies*.

[20] Elhorst, J.P (2009), "Spatial panel data models", in M.M. Fischer & A.Getis (Eds), *Handbook of Applied Spatial Analysis*, pp. 377-407.

[21] Elhorst, J.P. (forthcoming), "Matlab Software for Spatial Panels", *International Regional Science Review*.

[22] Fearon, J. D. and Laitin, D. (2003), "Ethnicity, Insurgency, and Civil War", *American Political Science Review* 97(1), pp. 75-90.

[23] Fotheringham, A.S. and Wong, D. (1991), "The modifiable areal unit problem in multivariate statistical analysis", *Environment and Planning* A 23, 1025-1044.

[24] Gleditsch, N. P., Owen, T., Furlong, K. and Lacina, B. (2006), "Conflicts over Shared Rivers: Resource Wars or Fuzzy Boundaries?", *Political Geography* 25(4), pp. 361–382.

[25] Hernández-Díaz, L., R. Laprise, L. Sushama, A. Martynov, K. Winger and B. Dugas (forthcoming), "Climate simulation over CORDEX Africa domain using the fifth-generation Canadian Regional Climate Model (CRCM5).", *Climate Dynamics.*

[26] Herschell, I. ad Grossman, H. (1991), "A General Equilibrium Model of Insurrections", *American Economic Review* 81(49), pp. 912-921.

[27] Heywood, I., S.Cornelius and S. Carver (1998), *Introduction to Geographical Information Systems*. New York: Addison Wesley Longman.

[28] Hsiang, S.M. (2010), "Temperatures and cyclones strongly associated with economic production in the Caribbean and Central America", *Proceedings of the National Academy of Sciences*, 107 15367-15372.

[29] Hughes , G. (2012) "Implementing procedures for spatial panel econometrics in Stata", mimeo.

[30] King, G. and L. Zheng (2001), "Logistic Regression in Rare Events Data", *Political Analysis*, 137-163.

[31] Kudamatsu, M., T. Persson and D. Strömberg (2012), "Weather and Infant Mortality in Africa", CEPR Discussion Paper 9222.

[32] Larrick, R.P., T.A. Timmerman, A.M. Carton and J. Abrevaya (2011), "Temper, Temperature, and Temptation", Psychological Science, 22, 423-428.

[33] Le Sage, J..P., and R.K. Pace (2009), *Introduction to spatial econometrics*. Boca Raton, US:CRC Press Taylor & Francis Group.

[34] Maccini, S., and D. Yang. (2009), "Under the Weather: Health, Schooling, and Socioeconomic Consequences of Early-life Rainfall.", *American Economic Review*, 99(3): 1006-1026.

[35] Manski, C. (2003), "Identification of Endogenous Social Effects: The Reflection Problem", *The Review of Economic Studies*, Vol. 60, No. 3.

[36] Michalopoulos, S. (2012), "The Origins of Ethnilinguistic Diversity", *American Economic Review*, 102(4), 1508-1539.

[37] Michalopoulos, S., and E.Papaioannou (2012), "The Long-Run Effects of the Scramble for Africa," NBER working paper 17620.

[38] Miguel, E., S. Satyanath, and E. Sergenti (2004), "Economic Shocks and Civil Conflict: An Instrumental Variables Approach", *Journal of Political Economy*, Vol. 112, pp. 725-753.

[39] Monfreda, C., N. Ramankutty and J.A. Foleyl (2008), "Farming the planet: Geographic Distribution of Crop Areas, Yields, Physiological Types, and Net Primary Production in the Year 2000 ", *Global Biochemical Cycles*.

[40] Montalvo, J.G., and M. Reynal-Querol (2005), "Ethnic Polarization, Potential Conflict and Civil War", *American Economic Review*, 95, 796-816.

[41] Nordhaus, W. D., Azam, Q., Corderi, D., Hood, K., Victor, N. M., Mohammed, M., Miltner, A. & Weiss, J. (2006), "The G-Econ database on gridded output: Methods and data", Yale University.

[42] Parent, O. and J.P.Le Sage (2009), "Spatial Dynamic Panel Data Models with Random Effects", mimeo.

[43] Portmann, F. T., S. Siebert and P.Döll. (2010), "MIRCA2000 – Global monthly irrigated and rainfed crop areas around the year 2000: A new high-resolution data set for agricultural and hydrological modeling", *Global Biogeochemical Cycles*, 24, GB 1011.

[44] Raleigh, C., A.Linke and H.Hegre and J.Karlsen. (2010), "Introducing ACLED-Armed Conflict Location and Event Data", *Journal of Peace Research* 47(5) 1-10.

[45] Schlenker, W. and D.B. Lobell (2010), "Robust Negative Impacts of Climate Change on African Agriculture", *Environ. Res. Lett.* 5 (2010).

[46] Schlenker, W., an M. Roberts (2008), "Estimating the Impact of Climate Change on Crop Yields: The Importance of Nonlinear Temperature Effects", NBER Working Paper 13799.

[47] U.S. Geological Survey (2005). Mineral Resources Data System: U.S. Geological Survey, Reston, Virginia.

[48] Vanden Eynde, O. (2011), "Targets of Violence: Evidence from India's Naxalite Conflict", mimeo, Paris School of Economics.

[49] Vicente-Serrano S.M., Beguería S., López-Moreno J.I., Angulo M., El Kenawy A. (2010), "A global 0.5° gridded dataset (1901-2006) of a multiscalar drought index considering the joint effects of precipitation and temperature", *Journal of Hydrometeorology* 11(4), 1033-1043, DOI: 10.1175/2010JHM1224.1.

[50] Weidmann, N. B., J. K. Rød and L.-E. Cederman (2010). "Representing Ethnic Groups in Space: A New Dataset". *Journal of Peace Research*, in press.

7 Appendix

7.1 Derivation of the likelihood for dynamic spatial panels[13]

Consider the following dynamic, spatial, random effects model with N cross-sectional units and T time periods:

$$y_t = \phi y_{t-1} + \rho W y_t + i_N \alpha + x_t \beta + \eta_t \tag{1}$$

with $\eta_t = \mu_t + \varepsilon_t$, where $y_t = (y_{1t,}\ ...,\ y_{Nt})'$ is the $N \times 1$ vector of observations for the t-th time period, α is the intercept, i_N is an $N \times 1$ column vector of ones, x_t is the $N \times k$ matrix of non-stochastic regressors and μ is an $N \times 1$ vector of random effects, with $\mu_i \sim N(0, \sigma_\mu^2)$. The random terms ε_t are i.i.d. with zero mean and a variance $\sigma_\varepsilon^2 I_N$, and μ is assumed to be uncorrelated with ε_t. W is a row-normalized, symmetric $N \times N$ spatial weighting matrix with zeros on the diagonal, whose eigenvalues are denoted as $\varpi_i, i = 1, ..., N$. For simplicity spatial lags of the covariates are not explicitly included in (1), but they could be part of matrix x_t .

The basic idea is to remove the two sources of autocorrelation by combining two transformations: a space filter to remove the spatially autoregressive term and a time filter à la Prais-Winsten to remove the temporal autoregressive one.

Define first the space filter as the $N \times N$ matrix

$$B = I_N - \rho W \tag{2}$$

To see how this transformation removes the spatial autoregressive term, suppose that $\phi = 0$ and apply this filter to equation (1):

$$B y_t = i_N \alpha + x_t \beta + \eta_t \tag{3}$$

Now define the time filter as the $T \times (T+1)$ matrix

$$C = \begin{bmatrix} -\phi & 1 & 0 & ... & 0 \\ \vdots & \ddots & \ddots & \ddots & \vdots \\ 0 & ... & ... & -\phi & 1 \end{bmatrix} \tag{4}$$

To see how this transformation removes the temporal autoregressive term, consider the $(T+1) \times 1$ vector of observations for the i-th cross-sectional unit $y_i = (y_{i0,}\ ...,\ y_{iT})'$. Similarly, let $x_i = (x_{i1,}\ ...,\ x_{iT})'$ be the $T \times k$ vector of covariates observed in the i-th

[13] This subsection draws upon Parent and Le Sage (2009).

cross-sectional unit and $\eta_i = (\eta_{i0,} ..., \eta_{iT})'$ a vector of errors. Further assume that $\rho = 0$. Applying the filter to y_i one obtains:

$$Cy_i = i_T\alpha + x_i\beta + \eta_i \tag{5}$$

Note that we are assuming that y_0 is given. This considerably simplifies the computational complexity of the estimation and has been shown to have little effect on the estimates when T is not too small.

The space-time filter proposed by Parent and LeSage is given by the Kronecker product of matrices C and B. Set $Y = (y_0', ..., y_T')'$ and $X = (x_1', ..., x_T')'$ and apply the filter to the entire vector of observations. One obtains:

$$(C \otimes B)Y = X\beta + i_{NT}\alpha + \eta \tag{6}$$

with $\eta \sim N(0, \Omega)$.

Since the random effects are integrated out, the $NT \times NT$ variance-covariance matrix can be shown to be equivalent to

$$\Omega = \sigma_\mu^2(J_T \otimes I_N) + \sigma_\varepsilon^2[I_T \otimes I_N] \tag{7}$$

with $J_{T+1} = i_{T+1}i_{T+1}'$.

This allows to write down the log-likelihood for the complete sample size of T for the model defined in (1) as

$$\ln L_T(\xi) = -\frac{NT}{2}\ln(2\pi) - \frac{1}{2}\ln|\Omega| + T\sum_{i=1}^{N}\ln[(1-\rho\varpi_i)] - \frac{1}{2}\eta'\Omega^{-1}\eta \tag{8}$$

where $\xi = (\beta', \alpha, \sigma_\varepsilon^2, \sigma_\mu^2, \phi, \rho)$.

7.2 The Standardized Precipitation-Evapotranspiration Index (SPEI)

Most studies related to drought analysis and monitoring systems have resorted to the Palmer Drought Severity Index (PDSI), based on a soil water balance equation, or the Standardized Precipitation Index (SPI), based on precipitation. One of the limitations of the PSDI index is its fixed temporal scale (between 9 and 12 months), and an autoregressive property by which PSDI values are affected by the conditions up to four years in the past (Vicente Serrano et al., 2010). Precipitation-based drought indices like SPI, on the other hand, assume that temperature and potential evapotranspiration (PET) have

negligible variability compared to precipitation. This makes such indexes unsuitable to identify the role of global warming in future drought conditions.

Our manual recalculation of SPEI uses the R routines developed by Vicente Serrano et al. (2010). Due to the probabilistic nature of the SPEI index, it is recommended to use the longest sample possible in its computation. We thus consider use the entire ERA-Interim available sample 1979-2011. The computation involves the following steps.

1) Compute climatic water balance, defined at the monthly level as the difference D between precipitation and potential evapotranspiration (PET).

Since no direct data on PET is usually available, SPEI is based on an approximation. A number of equations exist to model PET based on available data. In our 1979-2011 sample we make use of the FAO-56 Penman-Monteith equation described in Allen et al. (1998), which is recommended by FAO as the best method for determining reference evapotranspiration. The original parameterization is used, corresponding to a short reference crop of 0.12 m height:

$$PET = \frac{0.408(R_n - G) + \gamma \frac{900}{T+273} u_2 (e_s - e_a)}{\Delta + \gamma(1 + 0.34 u_2)}$$

where R_n is the net radiation at crop surface, G is the soil heat flux density, T is the mean daily air temperature at 2m height, e_S is saturation water pressure, e_a is actual vapor pressure, Δ is the slope of the vapor pressure curve and γ is the psychometric constant. Given that many of these inputs are seldom available, chap. 3 of Allen et al. (1998) provides methods to compute the missing variables based on available data. For instance, incoming solar radiation can be estimated based on sunshine duration or percent cloud cover. Similarly, saturation water pressure can be estimated from the dewpoint temperature. If unavailable, the atmospheric surface pressure required for computing the psychrometric constant can be assumed to be constant. The inputs we use to approximate the Penman equation in our 1979-2011 sample are: average temperature, average maximum and minimum daily temperatures, dewpoint temperature, cloud cover, sunshine duration and wind speed.

In our exercise with future climate projections, due to more limited data availability, PET is approximated with the less demanding Hargreaves equation (Hargreaves, 1994). For consistency, the water balance threshold for the definition of SPEI Shock Growing Season in the 1997-2011 sample is obtained with a Hargreaves-based PET too. The Hargreaves equation is

$$PET = 0.00203 \cdot R_a \cdot (\frac{(T_{\max} + T_{\min})}{2} + 17.8) \cdot (T_{\max} - T_{\min})^{0.5}$$

where R_a is mean external radiation, $T_{\max}$ and $T_{\min}$ are the mean daily maximum and minimum temperature at 2m height. Mean external radiation is estimated from the latitude and the month of the year.

2) The calculated difference D between precipitation and PET is aggregated at different time scales, as done for the SPI. This is achieved by applying a kernel function to the data, which allows incorporating information of previous time steps into the calculation of the current step. We use a Gaussian kernel, allowing data from the past to have a decreasing influence in the current step as the temporal lag between current and past steps increases.

3) Finally, the time series is standardized according to a Log Logistic distribution, whose parameters are estimated by the L-moment procedure. The probability distribution function of D according to the Log-logistic is

$$F(x) = \left[1 + \left(\frac{\alpha}{x - \gamma}\right)^{\beta}\right]^{-1}$$

SPEI is calculated as the standardized values of $F(x)$. By construction it has mean 0 and standard deviation 1 in a given location over the entire sample period - in our case 1979-2011.

Bibliography

Allen R. G., Smith M., Pereira L. S., Perrier A.(1994), "Crop evapotranspiration - Guidelines for computing crop water requirements", FAO Irrigation and drainage paper 56.

Hargreaves G.H. (1994), "Defining and using reference evapotranspiration", *Journal of Irrigation and Drainage Engineering* 120: 1132–1139.

Table 1: Summary statistics

A: Cross sectional sample	No. Obs.	Mean	Std Dev
Fraction of years with conflict	2669	0.171	0.252
Shared	2669	0.252	0.434
Border	2669	0.050	0.218
Area, in km^2	2669	10926.7	2577.3
Elevation, in m	2669	314.861	269.567
Rough	2669	0.093	0.102
Distance to river, in km	2669	628.0	476.1
Road	2669	0.241	0.428
Minerals	2669	0.210	0.408
ELF	2669	0.203	0.240
B: Panel sample			
ANY EVENT	37425	0.170	0.376
BATTLE	37425	0.098	0.297
CIVILIAN	37425	0.098	0.297
RIOT	37425	0.056	0.231
REBEL	37425	0.029	0.168
SPEI	37425	-0.089	0.575
SPEI Shock, Growing Season	37425	0.105	0.188
SPEI Growing Season, Main Crop	37425	-0.022	0.362
Rain	37425	65.11	69.13
Rain Growing Season, Main Crop	37425	51.58	63.86
Temperature, abs dev	37425	0.782	0.203
Temperature abs dev, Growing Season, Main Crop	37425	0.332	0.320

Table 2: Conflict incidence, cross section

Dependent variable: fraction of years 1997-2011 with at least one conflict event

	(1)	(2)	(3)	(4)	(5)	(6)
	Model I OLS		Model II OLS		Model III MLE	
W · Y					0.0467***	0.0237***
					(0.0039)	(0.0045)
Shared	0.0463**	0.0379***	0.0348***	0.0273**	0.0492***	0.0340***
	(0.0180)	(0.0128)	(0.0129)	(0.0118)	(0.0116)	(0.0099)
Border	0.002	0.0021	-0.0126	-0.0173	-0.0119	-0.0070
	(0.0229)	(0.0181)	(0.0161)	(0.0160)	(0.0181)	(0.0162)
Area[(a)]	0.005	0.000	0.0037	0.0028	0.0033	-0.0008
	(0.0031)	(0.0025)	(0.0047)	(0.0049)	(0.0020)	(0.0023)
Elevation[(a)]	-0.102***	-0.0705*	-0.280**	-0.337***	-0.0681***	-0.0759***
	(0.0362)	(0.0397)	(0.125)	(0.128)	(0.0181)	(0.0241)
Rough	0.480***	0.377***	0.235**	0.279***	0.462***	0.430***
	(0.113)	(0.106)	(0.098)	(0.0833)	(0.0597)	(0.0652)
Distance to river[(b)]	-0.0068***	-0.0058**	0.0058	-0.0017	-0.0089***	-0.005**
	(0.0025)	(0.0027)	(0.0046)	(0.0043)	(0.0013)	(0.0019)
Road	0.101***	0.0932***	0.112***	0.106***	0.117***	0.0949***
	(0.0210)	(0.0164)	(0.0160)	(0.0152)	(0.0130)	(0.0127)
ELF	0.0793**	0.0514*	0.0337	0.0393*	0.0735***	0.0422**
	(0.0325)	(0.0265)	(0.0233)	(0.0225)	(0.0216)	(0.0201)
Minerals	0.0649***	0.0616***	0.0499***	0.0486***	0.0616***	0.0560***
	(0.0160)	(0.0138)	(0.0110)	(0.0117)	(0.0126)	(0.0113)
W·Shared			0.00231	-0.0009	-0.0067*	-0.0005
			(0.0045)	(0.0033)	(0.0035)	(0.0033)
W·Border			0.0117	0.0099	0.0132**	0.0122**
			(0.0098)	(0.0072)	(0.0063)	(0.0055)
W·Area[(a)]			0.0005	-0.0008	0.0000	0.0001
			(0.0011)	(0.0011)	(0.0004)	(0.0005)
W·Elevation[(a)]			0.0262	0.0401**	-0.0040	0.0010
			(0.0193)	(0.0183)	(0.0053)	(0.0074)
W·Rough			0.0462***	0.0145	-0.0260**	-0.0236
			(0.0169)	(0.0205)	(0.0125)	(0.0165)
W·Distance to river[(b)]			-0.0018***	-0.0006	0.0007**	0.0000
			(0.0007)	(0.0007)	(0.0003)	(0.0005)
W·Road			-0.0039	-0.0064	-0.0142***	0.0029
			(0.0038)	(0.0041)	(0.0034)	(0.0039)
W·ELF			0.0100	0.0047	0.0013	0.0022
			(0.0087)	(0.0072)	(0.0057)	(0.006)
W·Minerals			0.0091*	0.0111**	0.0032	0.0056
			(0.005)	(0.0045)	(0.0040)	(0.0038)
Country FE		X		X		X
Observations	2,669	2,669	2,669	2,669	2,669	2,669
R-squared	0.436	0.587	0.446	0.630	0.184	0.421

(a) Coefficient and std error multiplied by 10^3 (b) Coefficient and std error multiplied by 10^2

Standard errors in parenthesis corrected for spatial dependence, following Conley (1999).

* p<0.01, ** p<0.05, * p<0.1. W = binary contiguity matrix, cutoff 180 km.

Table 3: Conflict incidence and climate, panel

Dependent variable (Y) = 1 if conflict event in year t (ANY EVENT)

	(1)	(2)	(3)
	Model I OLS	Model II OLS	Model III MLE
Y, t-1			0.332***
			(0.0049)
W · Y			0.0451***
			(0.0010)
SPEI	0.0077	0.0263*	0.0103
	-0.0054	(0.0136)	(0.0123)
SPEI, t-1	-0.0102*	0.0124	-0.0005
	-0.0057	(0.0138)	(0.0122)
SPEI, t-2	0.0032	0.0056	0.0043
	-0.0056	(0.0140)	(0.0117)
SPEI Shock Growing Season	0.0469***	0.0272	0.0103
	(0.0179)	(0.0195)	(0.0190)
SPEI Shock Growing Season, t-1	0.0550***	0.0499**	0.0401**
	(0.0180)	(0.0212)	(0.0196)
SPEI Shock Growing Season, t-2	0.0594***	0.0458**	0.0407**
	(0.0180)	(0.0213)	(0.0194)
W · SPEI		-0.0024	0.000
		(0.0021)	(0.0018)
W · SPEI, t-1		-0.0034	-0.0010
		(0.0021)	(0.0018)
W · SPEI, t-2		-0.0001	-0.0005
		(0.0022)	(0.0018)
W · SPEI Shock Growing Season		0.0060	0.0025
		(0.0041)	(0.0033)
W · SPEI Shock Growing Season, t-1		0.0022	-0.0029
		(0.0042)	(0.0034)
W · SPEI Shock Growing Season, t-2		0.0047	-0.0031
		(0.0043)	(0.0034)
Observations	37,425	37,425	37,425
R-squared	0.327	0.353	0.347

Notes: Each observation is a cell/year. All regressions include controls listed in table 2, country and year fixed effects. W = binary contiguity matrix, cutoff 180 km.

Standard errors in parenthesis. Cols. 1, 2 corrected for spatial and serial correlation. Col. 3 corrected for clustering at the cell level. *** p<0.01, ** p<0.05, * p<0.1

Table 4: Sensitivity to different spatial matrices

Dependent variable (Y) = 1 if conflict event in year t (ANY EVENT)

	(1)	(2)	(3)	(4)
	Binary contiguity matrix			
	180 km	290 km	450 km	600 km
Y, t-1	0.332***	0.330***	0.339***	0.350***
	(0.0049)	(0.00493)	(0.00495)	(0.00496)
W · Y	0.0451***	0.0248***	0.0122***	0.00707***
	(0.0010)	(0.000543)	(0.000298)	(0.000201)
SPEI	0.0103	0.00875	0.00581	0.00658
	(0.0123)	(0.00957)	(0.00754)	(0.00645)
SPEI, t-1	-0.0005	-0.00110	-0.00648	-0.00960
	(0.0122)	(0.00972)	(0.00761)	(0.00662)
SPEI, t-2	0.0043	0.00448	0.00404	0.00800
	(0.0117)	(0.00907)	(0.00716)	(0.00616)
SPEI Shock Growing Season	0.0103	0.0142	0.0177	0.0215
	(0.0190)	(0.0172)	(0.0158)	(0.0150)
SPEI Shock Growing Season, t-1	0.0401**	0.0266	0.0119	0.00384
	(0.0196)	(0.0183)	(0.0170)	(0.0160)
SPEI Shock Growing Season, t-2	0.0407**	0.0306*	0.0400**	0.0383**
	(0.0194)	(0.0181)	(0.0166)	(0.0156)
W · SPEI	0.000	-2.57e-05	2.46e-05	-1.56e-05
	(0.0018)	(0.000623)	(0.000221)	(0.000118)
W · SPEI, t-1	-0.0010	-0.000337	6.03e-05	0.000131
	(0.0018)	(0.000643)	(0.000227)	(0.000121)
W · SPEI, t-2	-0.0005	-0.000234	-0.000140	-0.000166
	(0.0018)	(0.000598)	(0.000214)	(0.000115)
W · SPEI Shock Growing Season	0.0025	0.000555	1.37e-05	-0.000170
	(0.0033)	(0.00140)	(0.000610)	(0.000364)
W · SPEI Shock Growing Season, t-1	-0.0029	-0.000513	0.000390	0.000490
	(0.0034)	(0.00143)	(0.000634)	(0.000388)
W · SPEI Shock Growing Season, t-2	-0.0031	-0.00100	-0.00116*	-0.000884**
	(0.0034)	(0.00146)	(0.000653)	(0.000392)
Observations	37,425	37,425	37,425	37,425
R-squared	0.347	0.347	0.343	0.341

Notes: Each observation is a cell/year. All regressions include controls listed in table 2, country and year fixed effects. Estimation by MLE. Standard errors corrected for clustering at the cell level.
*** p<0.01, ** p<0.05, * p<0.1

Table 5: Sensitivity to different spatial resolutions

Panel A: 2x2 cells

Dependent variable (Y) = 1 if conflict event in year t (ANY EVENT).

	Model I - OLS				Model III - MLE			
	avg. coefficient	coefficient std. dev.	avg. std. error	no. panels 10% significant	avg. coefficient	coefficient std. dev.	avg. std. error	no. panels 10% significant
Y, t-1					0.3825	0.0150	0.0100	4
W · Y					0.0585	0.0013	0.0021	4
SPEI	0.0081	0.0016	0.0082	0	0.0041	0.0081	0.0100	0
SPEI, t-1	-0.0094	0.0012	0.0090	0	-0.0025	0.0037	0.0105	0
SPEI, t-2	-0.0029	0.0019	0.0086	0	0.0055	0.0026	0.0103	0
SPEI Shock Growing Season	0.0597	0.0055	0.0282	4	0.0218	0.0128	0.0267	0
SPEI Shock Growing Season, t-1	0.0643	0.0056	0.0270	4	-0.0014	0.0155	0.0276	0
SPEI Shock Growing Season, t-2	0.0588	0.0075	0.0272	4	0.0460	0.0167	0.0282	2
W · SPEI					0.0008	0.0015	0.0018	0
W · SPEI, t-1					-0.0013	0.0007	0.0019	0
W · SPEI, t-2					-0.0010	0.0005	0.0018	0
W · SPEI Shock Growing Season					0.0005	0.0022	0.0051	0
W · SPEI Shock Growing Season, t-1					0.0022	0.0024	0.0055	0
W · SPEI Shock Growing Season, t-1					-0.0070	0.0024	0.0056	0
Average nr of obs	8051				8033			
Average R squared	0.559				0.559			

Panel B: 3x3 cells

Dependent variable (Y) = 1 if conflict event in year t (ANY EVENT).

	Model I - OLS				Model III - MLE			
	avg. coefficient	coefficient std. dev.	avg. std. error	no. of panels in which 10% significant	avg. coefficient	coefficient std. dev.	avg. std. error	no. of panels in which 10% significant
Y, t-1					0.4550	0.0230	0.0134	9
W · Y					0.0598	0.0023	0.0030	9
SPEI	0.0103	0.0042	0.0089	1	0.0144	0.0065	0.0094	4
SPEI, t-1	-0.0066	0.0040	0.0096	0	-0.0153	0.0095	0.0107	5
SPEI, t-2	-0.0011	0.0024	0.0094	0	0.0176	0.0007	0.0098	5
SPEI Shock Growing Season	0.0609	0.0132	0.0332	4	0.0412	0.0083	0.0309	2
SPEI Shock Growing Season, t-1	0.0787	0.0107	0.0321	9	-0.0157	0.0236	0.0295	1
SPEI Shock Growing Season, t-2	0.0655	0.0154	0.0314	7	0.0624	0.0329	0.0296	6
W · SPEI					-0.0019	0.0010	0.0018	1
W · SPEI, t-1					0.0022	0.0019	0.0021	3
W · SPEI, t-2					-0.0040	0.0010	0.0019	7
W · SPEI Shock Growing Season					-0.0059	0.0024	0.0060	2
W · SPEI Shock Growing Season, t-1					0.0100	0.0057	0.0064	4
W · SPEI Shock Growing Season, t-2					-0.0159	0.0056	0.0078	8
Average nr of obs	4158				4158			
Average R squared	0.635				0.664			

Notes:

Regressions include controls listed in table 2, country and year fixed effects. OLS standard errors corrected for spatial and serial correlation. MLE standard errors corrected for clustering at the cell level. *** p<0.01, ** p<0.05, * p<0.1

Panel A: Results of the estimation of models I and III in 4 possible panels of 2x2 cells. W = binary contiguity matrix, cutoff 390 km.

Panel B: Results of the estimation of models I and III in 9 possible panels of 3x3 cells. effects. W = binary contiguity matrix, cutoff 490 km.

Table 6: Conflict incidence and other climate indicators

Dependent variable (Y) = 1 if conflict event in year t (ANY EVENT)

	(1)	(2)	(3)	(4)	(5)	(6)
		Log rain			**Temperature absolute deviation**	
	Model I	Model II	Model III	Model I	Model II	Model III
Y, t-1			0.331***			0.330***
			(0.0049)			(0.0049)
W · Y			0.0450***			0.0449***
			(0.0010)			(0.0010)
Climate	0.0007	0.0003	0.000	-0.01	0.0026	0.0206
	(0.0004)	(0.0006)	(0.0005)	(0.0167)	(0.0291)	(0.0250)
Climate, t-1	-0.0005	0.0006	0.0005	0.0127	0.0039	0.0161
	(0.0004)	(0.0006)	(0.0006)	(0.0168)	(0.0309)	(0.0272)
Climate, t-2	0.0005	-0.0001	-0.0003	-0.0523***	-0.0270	-0.0097
	(0.0004)	(0.0006)	(0.0005)	(0.0169)	(0.0299)	(0.0267)
Climate, Growing Season Indicator	0.000	0.0005	0.0004	0.0533**	0.009	0.0063
	(0.0005)	(0.0005)	(0.0005)	(0.0208)	(0.0251)	(0.0234)
Climate, Growing Season Indicator, t-1	0.0008	-0.0002	-0.0004	0.0225	0.0400	0.0287
	(0.0005)	(0.0005)	(0.0005)	(0.0212)	(0.0257)	(0.0267)
Climate, Growing Season Indicator, t-2	-0.0001	0.0002	0.0003	0.0669***	0.0525**	0.0300
	(0.0005)	(0.0005)	(0.0005)	(0.0217)	(0.0267)	(0.0251)
W · Climate		0.000	0.000		-0.0042	-0.0047
		(0.0001)	(0.000)		(0.0049)	(0.0040)
W · Climate, t-1		-0.0002**	-0.0002**		0.0007	-0.00175
		(0.0001)	(0.0001)		(0.0051)	(0.0044)
W · Climate, t-2		0.0001	0.0002*		-0.0057	-0.0045
		(0.0001)	(0.000)		(0.0050)	(0.0041)
W · Climate, Growing Season Indicator		-0.0001	0.000		0.0121**	0.0037
		(0.0001)	(0.000)		(0.0048)	(0.004)
W · Climate, Growing Season Indicator, t-1		0.0002*	0.0002**		-0.0012	-0.0025
		(0.0001)	(0.0001)		(0.0049)	(0.0045)
W · Climate, Growing Season Indicator, t-2		-0.0001	-0.0001*		0.0062	0.0010
		(0.0001)	(0.000)		(0.0051)	(0.0042)
Observations	37,425	37,425	37,425	37,425	37,425	37,425
R squared	0.307	0.344	0.348	0.331	0.358	0.348

Notes: Each observation is a cell/year. All regressions include controls listed in table 2, country and year fixed effects. W = binary contiguity matrix, cutoff 180 km.

Standard errors in parenthesis. Cols. 1-2-4-5 corrected for spatial and serial correlation. Cols. 3-6 corrected for clustering at the cell level. *** p<0.01, ** p<0.05, * p<0.1

Table 7: Different types of conflict events, cross section

	Y = BATTLE			*Y = CIVILIAN*			*Y = RIOT*			*Y = REBEL*		
	(1)	(2)	(3)	(4)	(5)	(6)	(7)	(8)	(9)	(10)	(11)	(12)
	Model I	Model II	Model III	Model I	Model II	Model III	Model I	Model II	Model III	Model I	Model II	Model III
W · Y			0.0233***			0.0280***			0.0008			0.0190***
			(0.00450)			(0.0044)			(0.0050)			(0.0045)
Shared	0.0268***	0.0207**	0.0237***	0.0220**	0.0139	0.0184**	-0.00389	-0.00486	-0.0050	0.0138***	0.00916**	0.0101***
	(0.00952)	(0.00893)	(0.00722)	(0.00993)	(0.00913)	(0.0076)	(0.00786)	(0.00839)	(0.0066)	(0.00452)	(0.00401)	(0.0037)
Border	0.00525	-0.00747	-0.00361	0.00794	-0.00631	0.0001	-0.000239	-0.00494	-0.0011	-0.00168	-0.00657	-0.0034
	(0.0123)	(0.0110)	(0.0108)	(0.0135)	(0.0133)	(0.0117)	(0.0109)	(0.0115)	(0.0111)	(0.00547)	(0.00559)	(0.0052)
Area[(a)]	0.00344**	0.00413	0.00342**	0.00103	0.00385	0.0008	-0.00418**	0.00151	-0.0046***	-0.000623	-0.000785	-0.0006
	(0.00154)	(0.00353)	(0.00140)	(0.00168)	(0.00388)	(0.0016)	(0.00178)	(0.00353)	(0.0017)	(0.000863)	(0.00196)	(0.0009)
Elevation[(a)]	-0.0356	-0.138	-0.0388**	-0.0353	-0.186*	-0.0342**	-0.0214	-0.257***	-0.0210	-0.00281	-0.0606	-0.0026
	(0.0287)	(0.0919)	(0.0167)	(0.0273)	(0.0963)	(0.0164)	(0.0214)	(0.0844)	(0.0159)	(0.00991)	(0.0438)	(0.0073)
Rough	0.234**	0.203***	0.300***	0.322***	0.246***	0.364***	0.164***	0.0851	0.165***	0.0741	0.0712	0.0875***
	(0.0938)	(0.0682)	(0.0521)	(0.0886)	(0.0741)	(0.0535)	(0.0532)	(0.0598)	(0.0419)	(0.0541)	(0.0449)	(0.0310)
Distance to river[(b)]	-0.00211	-0.00184	-0.0016	-0.00368**	-0.00151	-0.0026*	-0.00312*	0.000452	-0.003**	-0.000168	-0.00249	0.0006
	(0.00178)	(0.00204)	(0.0012)	(0.00179)	(0.00282)	(0.0013)	(0.00185)	(0.00378)	(0.0014)	(0.000690)	(0.00167)	(0.0006)
Road	0.0446***	0.0584***	0.0479***	0.0571***	0.0671***	0.0610***	0.0693***	0.0756***	0.0676***	0.0169***	0.0171***	0.0174***
	(0.0108)	(0.0104)	(0.0083)	(0.0126)	(0.0123)	(0.0096)	(0.0120)	(0.0121)	(0.0100)	(0.00502)	(0.00493)	(0.0043)
ELF	0.0446**	0.0298*	0.0337**	0.0424**	0.0393**	0.0397***	0.0140	0.0250	0.0144	0.0124	0.0103	0.0104
	(0.0184)	(0.0153)	(0.0139)	(0.0202)	(0.0171)	(0.0145)	(0.0159)	(0.0165)	(0.0133)	(0.00864)	(0.00761)	(0.0066)
Minerals	0.0333***	0.0281***	0.0304***	0.0331***	0.0260***	0.0287***	0.0345***	0.0232***	0.0324***	0.0101**	0.00657	0.0089**
	(0.00865)	(0.00740)	(0.0077)	(0.00978)	(0.00859)	(0.0084)	(0.0101)	(0.00882)	(0.0084)	(0.00461)	(0.00400)	(0.0038)
W·Shared		-0.000346	-0.0014		-0.000395	-0.0007		-0.00171	0.0014		0.00114	0.0029**
		(0.00229)	(0.0025)		(0.00252)	(0.0025)		(0.00223)	(0.0021)		(0.000965)	(0.0014)
W·Border		0.00515	0.0084**		0.00475	0.0101**		0.00426	0.0050		-0.00281	0.0040**
		(0.00564)	(0.0039)		(0.00528)	(0.0041)		(0.00362)	(0.0037)		(0.00208)	(0.0018)
W·Area[(a)]		-3.02e-05	-0.0001		-0.00102	-0.0002		-0.00149*	0.0001		-0.000552	-0.0001
		(0.000787)	(0.0004)		(0.000893)	(0.0004)		(0.000802)	(0.0004)		(0.000435)	(0.0002)
W·Elevation[(a)]		0.0132	0.0024		0.0239*	-0.0018		0.0350***	-0.0054		0.0101*	-0.001
		(0.0131)	(0.0049)		(0.0140)	(0.0055)		(0.0118)	(0.0052)		(0.00575)	(0.0023)
W·Rough		0.00558	-0.0272**		0.0128	-0.0237*		0.00984	-0.0003		-0.00373	-0.0042
		(0.0180)	(0.0117)		(0.0159)	(0.0125)		(0.0103)	(0.0095)		(0.00590)	(0.0056)
W·Distance to river[(b)]		4.83e-05	0.000		-0.000353	-0.0001		-0.000629	0.0001		0.000345	-0.0002
		(0.000414)	(0.0004)		(0.000474)	(0.0004)		(0.000581)	(0.0004)		(0.000256)	(0.0002)
W·Road		-0.00583**	0.0032		-0.00578*	0.0007		-0.00450	0.0037		-0.00145	0.0028**
		(0.00273)	(0.0026)		(0.00306)	(0.0029)		(0.00277)	(0.0028)		(0.00119)	(0.0014)
W·ELF		0.00650	0.0030		0.00298	0.0016		-0.00557	-0.0031		0.000653	-0.0007
		(0.00495)	(0.0041)		(0.00536)	(0.0043)		(0.00381)	(0.00385)		(0.00197)	(0.0018)
W·Minerals		0.00559**	0.0024		0.00616**	0.0029		0.00949***	0.0066**		0.00316**	0.0014
		(0.00278)	(0.0027)		(0.00310)	(0.0028)		(0.00349)	(0.0026)		(0.00152)	(0.0012)
Observations	2,669	2,669	2,669	2,669	2,669	2,669	2,669	2,669	2,669	2,669	2,669	2,669
R-squared	0.538	0.600	0.433	0.531	0.585	0.431	0.329	0.364	0.245	0.408	0.483	0.374

Notes: Each observation is a cell. All regressions include country fixed effects. W = binary contiguity matrix, cutoff 180 km.

(a) Coefficient and std error multiplied by 10^3 (b) Coefficient and std error multiplied by 10^2. Standard errors in parenthesis corrected for spatial dependence, following Conley (1999).

Table 8: Different types of conflict events, panel

	Y = BATTLE			*Y = CIVILIAN*			*Y = RIOT*			*Y = REBEL*		
	(1)	(2)	(3)	(4)	(5)	(6)	(7)	(8)	(9)	(10)	(11)	(12)
	Model I	Model II	Model III	Model I	Model II	Model III	Model I	Model II	Model III	Model I	Model II	Model III
Y, t-1			0.274***			0.289***			0.335***			0.246***
			(0.0050)			(0.0050)			(0.0051)			(0.0054)
W · Y			0.0487***			0.0432***			0.0305***			0.0402***
			(0.0010)			(0.0011)			(0.0011)			(0.0011)
SPEI	0.0038	0.0194*	0.0096	0.0002	0.0042	-0.0047	0.0075**	0.0180*	0.0099	0.000	-0.0048	-0.0103
	(0.0044)	(0.0111)	(0.01)	(0.0042)	(0.0112)	(0.0099)	(0.0033)	(0.0100)	(0.0092)	(0.0023)	(0.0060)	(0.0066)
SPEI, t-1	-0.0135***	0.0022	-0.0061	-0.0036	-0.0055	-0.0076	-0.0001	0.0169*	0.0098	-0.0045*	-0.0066	-0.0012
	(0.0045)	(0.0111)	(0.0104)	(0.0044)	(0.0113)	(0.0104)	(0.0033)	(0.0102)	(0.0090)	(0.0024)	(0.0067)	(0.0067)
SPEI, t-2	-0.0052	0.0011	-0.0002	0.0006	0.0066	0.0097	0.004	0.0029	0.0023	-0.0017	-0.0104	-0.0061
	(0.0044)	(0.0113)	(0.0097)	(0.0045)	(0.0115)	(0.0097)	(0.0033)	(0.0100)	(0.0085)	(0.0026)	(0.0068)	(0.0067)
SPEI Shock Growing Season	0.0277*	-0.0038	-0.0106	0.0234*	-0.0040	-0.0082	-0.0014	0.0262**	0.0219*	0.0101	0.0149	0.0071
	(0.0148)	(0.0157)	(0.0163)	(0.0142)	(0.0156)	(0.0154)	(0.0098)	(0.0132)	(0.0122)	(0.0083)	(0.0102)	(0.0094)
SPEI Shock Growing Season, t-1	0.0404***	0.0500***	0.0456***	0.0253*	0.0192	0.0173	0.0008	0.005	-0.0050	0.0017	0.0104	0.0070
	(0.0151)	(0.0173)	(0.0174)	(0.0136)	(0.0175)	(0.0164)	(0.0097)	(0.0139)	(0.0135)	(0.0076)	(0.0107)	(0.0111)
SPEI Shock Growing Season, t-2	0.0365**	0.0148	0.0098	0.0203	0.0408**	0.0362**	0.0167	0.0246*	0.0311**	0.0025	0.0063	0.0023
	(0.0148)	(0.0183)	(0.0160)	(0.0138)	(0.0165)	(0.0161)	(0.0104)	(0.0147)	(0.0134)	(0.0072)	(0.0096)	(0.0100)
W · SPEI		-0.0020	-0.0007		-0.0001	0.0015		-0.0018	-0.0006		0.0008	0.0020**
		(0.0017)	(0.0014)		(0.0017)	(0.0015)		(0.0014)	(0.0013)		(0.001)	(0.001)
W · SPEI, t-1		-0.0026	0.000		0.0004	0.0007		-0.0026*	-0.0016		0.0002	-0.0004
		(0.0017)	(0.0015)		(0.0018)	(0.0015)		(0.0015)	(0.0013)		(0.0010)	(0.001)
W · SPEI, t-2		-0.0007	-0.0005		-0.0017	-0.0016		0.0001	0.000		0.0013	0.0004
		(0.0017)	(0.0014)		(0.0018)	(0.0014)		(0.0015)	(0.0012)		(0.0011)	(0.001)
W · SPEI Shock Growing Season		0.0077**	0.0042		0.0076**	0.0051*		-0.0046**	-0.0042**		-0.0001	0.0003
		(0.0034)	(0.0028)		(0.0031)	(0.0027)		(0.0023)	(0.0020)		(0.0018)	(0.0016)
W · SPEI Shock Growing Season, t-1		-0.0017	-0.0037		0.0026	-0.0019		0.000	0.0019		-0.0012	-0.0012
		(0.0034)	(0.0029)		(0.0033)	(0.0028)		(0.0025)	(0.0022)		(0.0018)	(0.0019)
W · SPEI Shock Growing Season, t-2		0.0058*	0.000		-0.0028	-0.004		-0.0007	-0.0021		0.0002	-0.0005
		(0.0035)	(0.0028)		(0.0033)	(0.0029)		(0.0025)	(0.0022)		(0.0018)	(0.0017)
Observations	37,425	37,425	37,425	37,425	37,425	37,425	37,425	37,425	37425	37,425	37,425	37,425
R-squared	0.234	0.263	0.286	0.255	0.283	0.308	0.153	0.174	0.232	0.131	0.156	0.205

Notes: Each observation is a cell/year. All regressions include controls listed in table 2, country and year fixed effects.
W = binary contiguity matrix, cutoff 180 km. Standard errors in parenthesis.
Cols. 1-2-4-5 corrected for spatial and serial correlation. Cols. 3-6 corrected for clustering at the cell level. *** p<0.01, ** p<0.05, * p<0.1

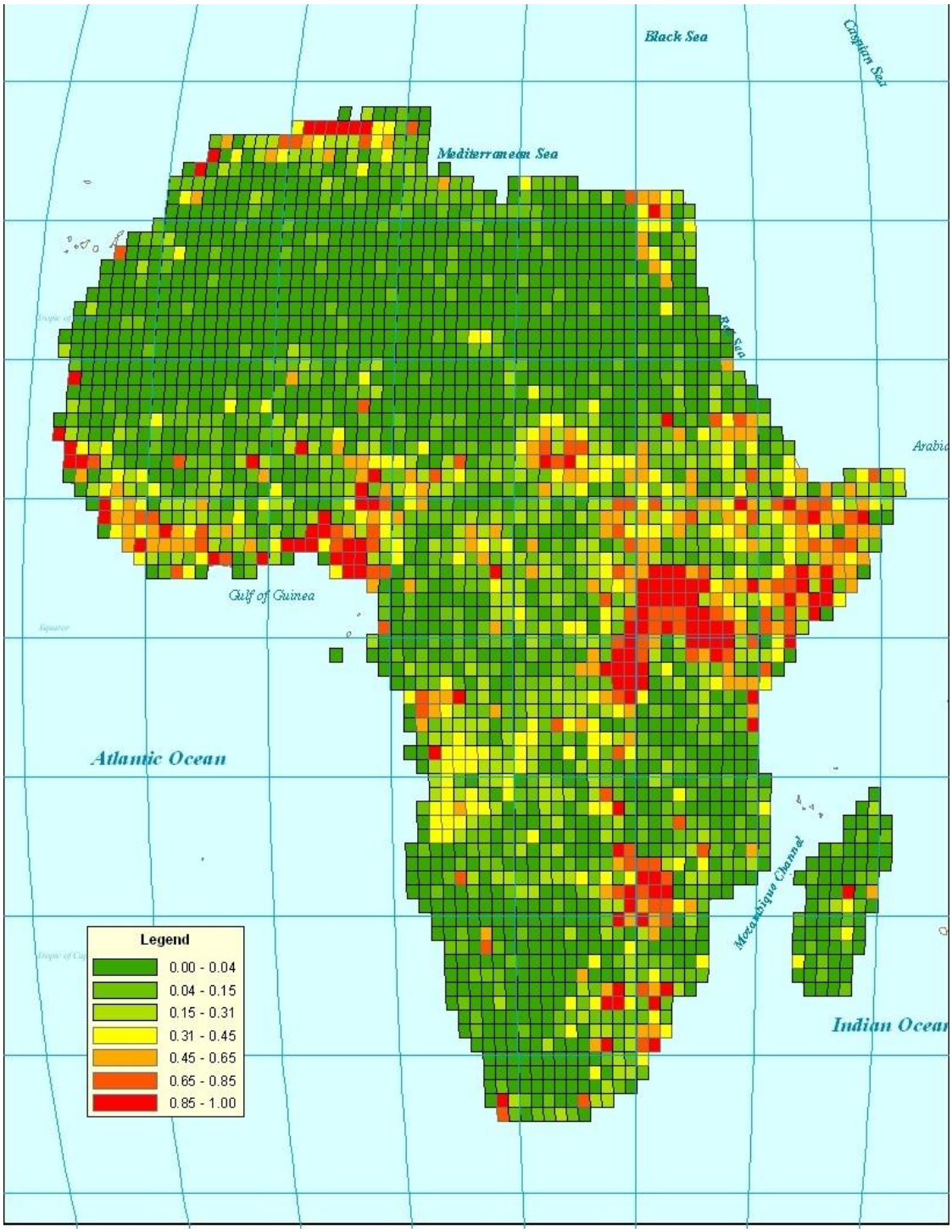

Figure 1:

Fraction of years with at least one conflict event (1997-2011)

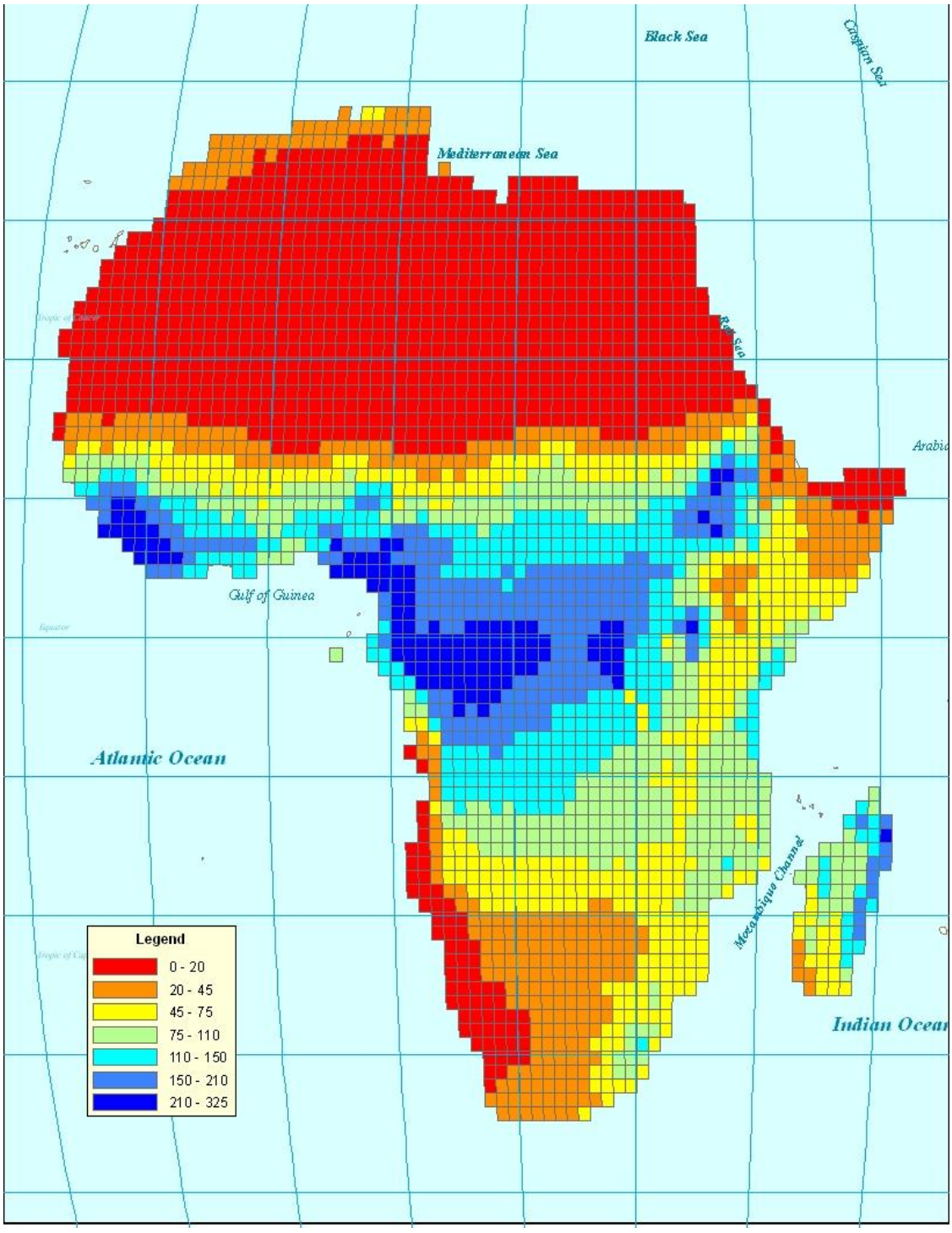

Figure 2:

Average yearly rainfall (in mm), 1997-2011

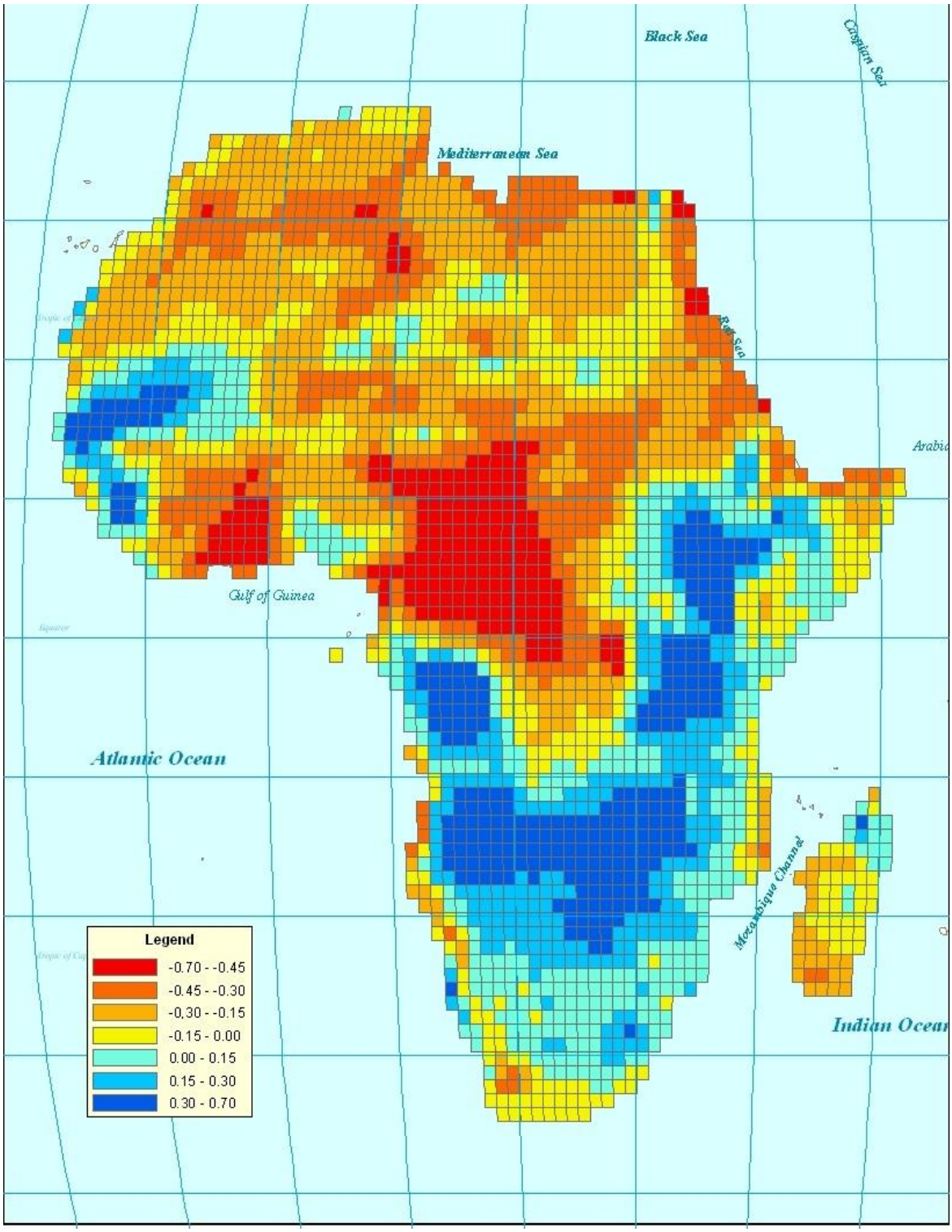

Figure 3:

Average SPEI, 1997 - 2011

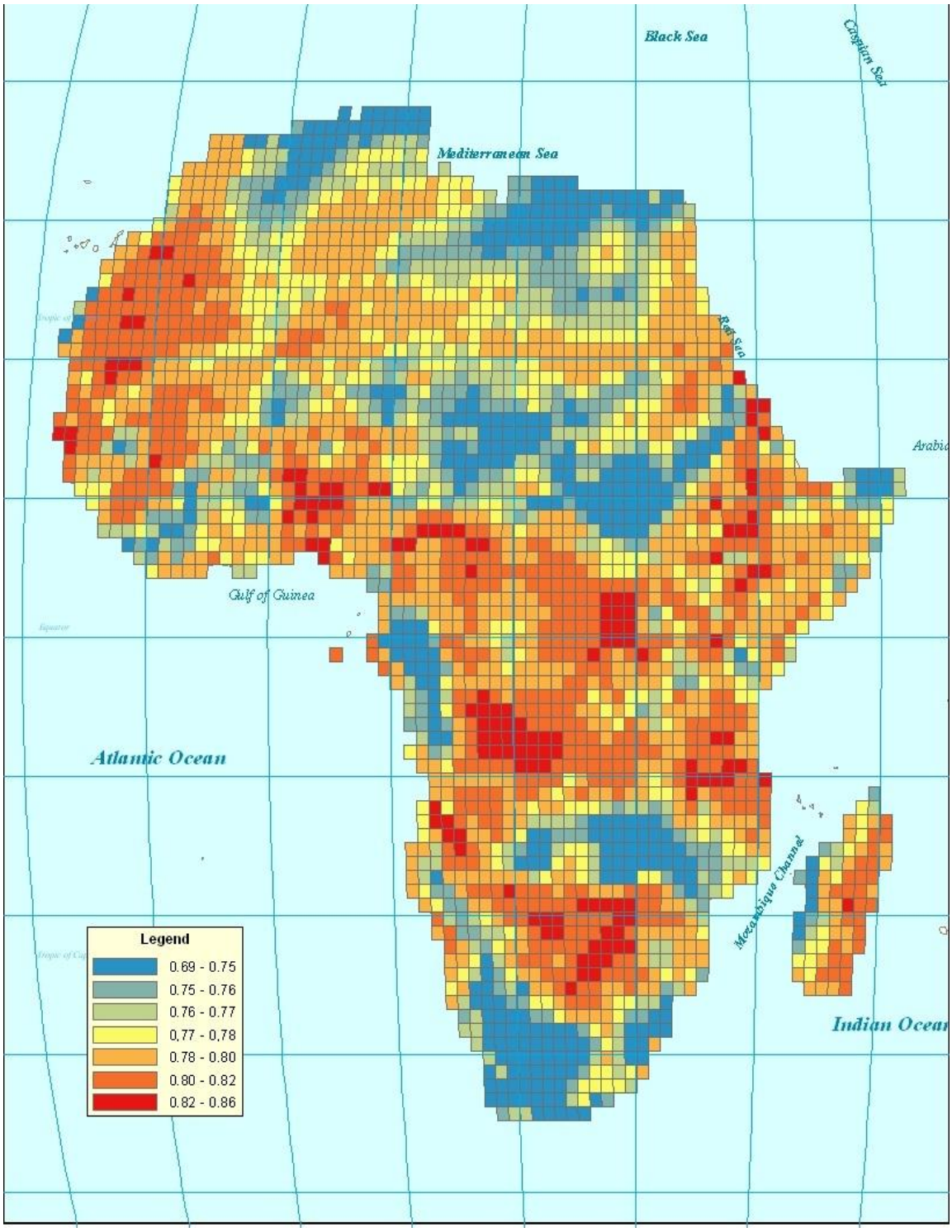

Figure 4:

Temperature, absolute deviation from cell mean, 1997 - 2011

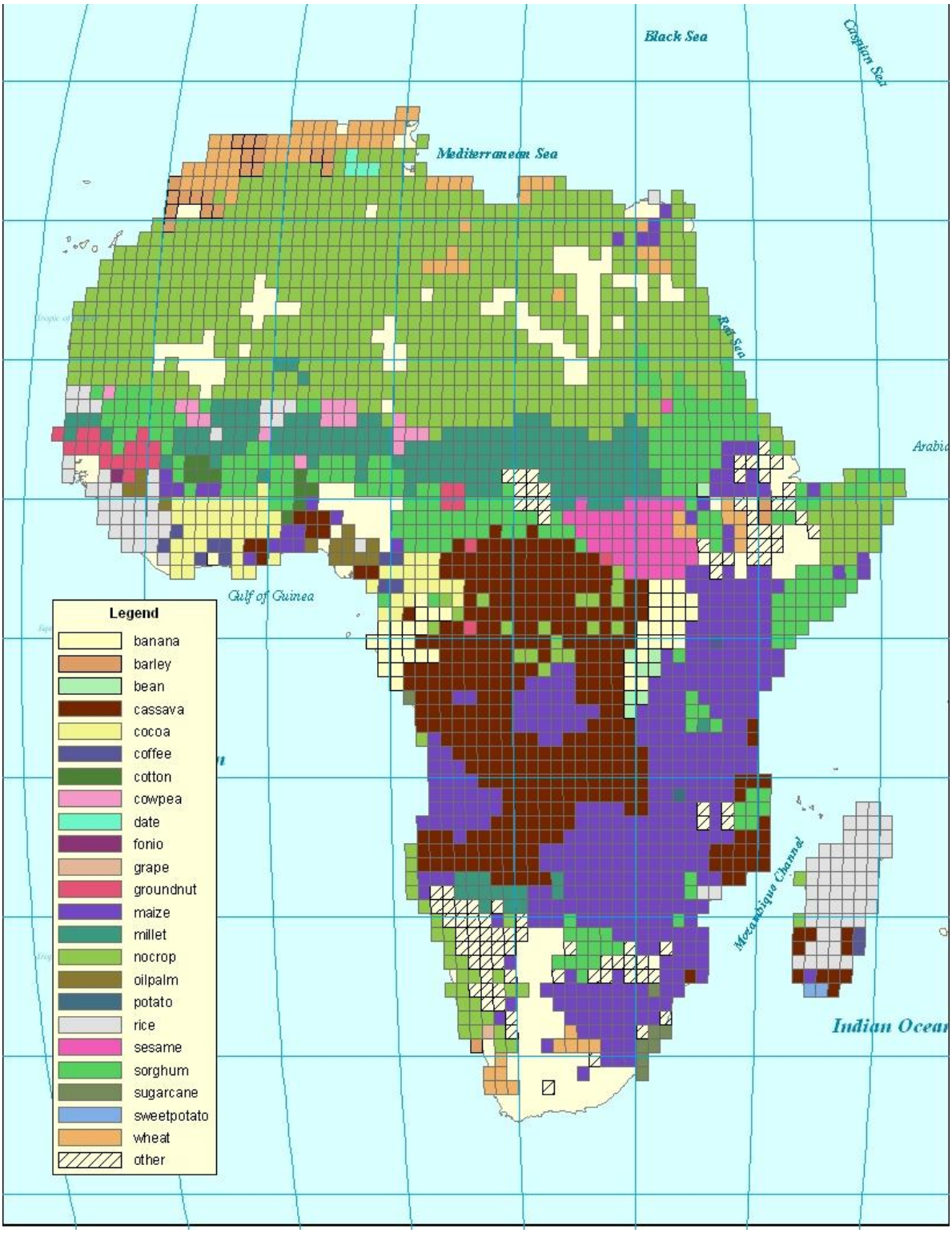

Figure 5:

Main crop

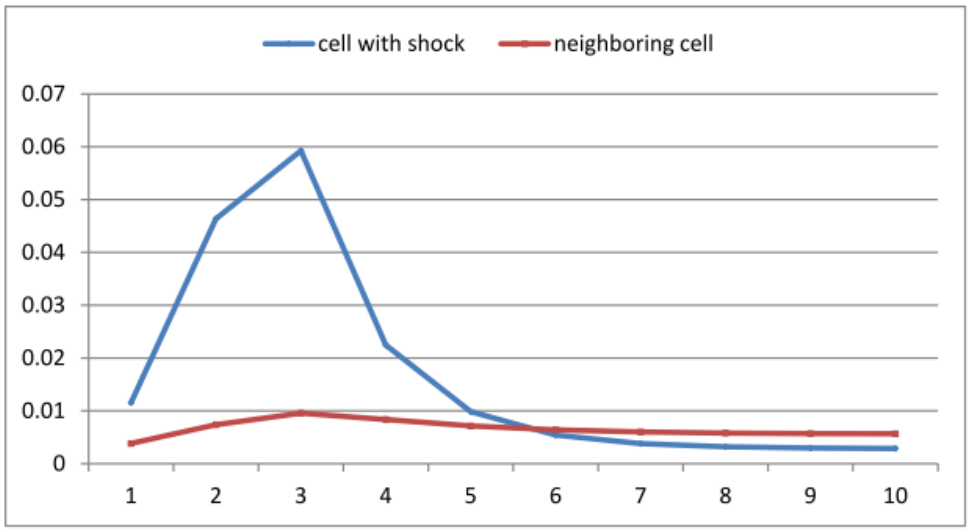

Figure 6:
Dynamic impact of a one-time SPEI shock on conflict incidence

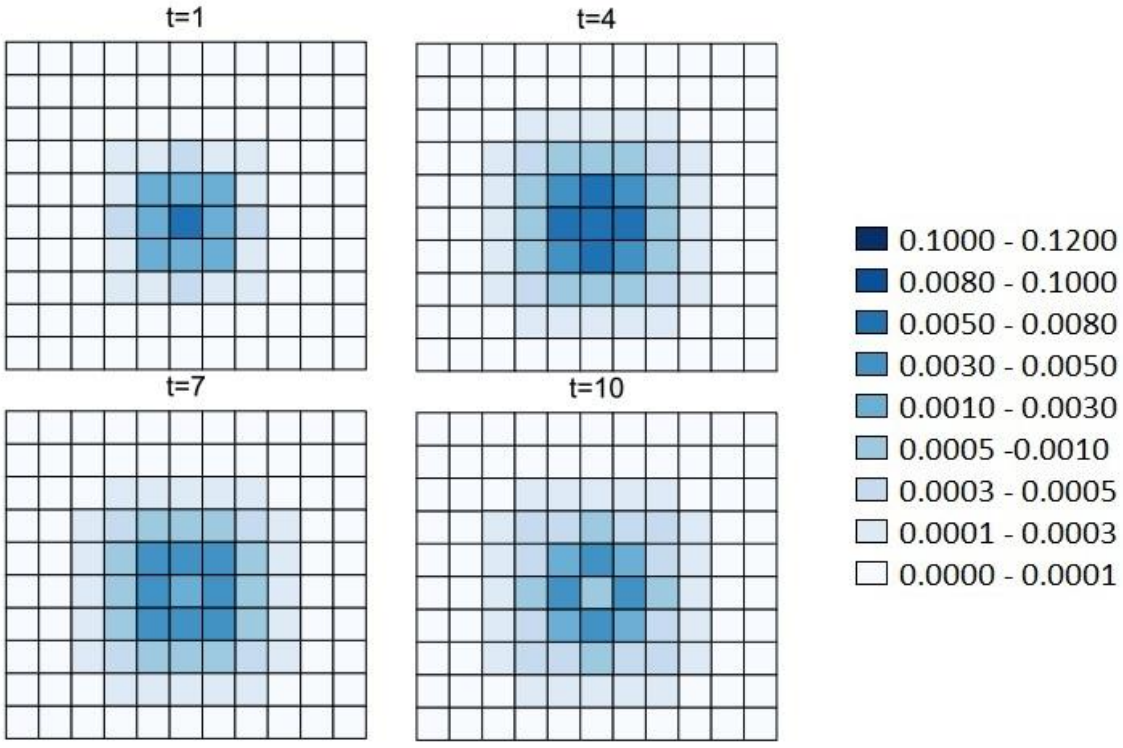

Figure 7:
Spatial impact of a one-time SPEI shock on conflict incidence

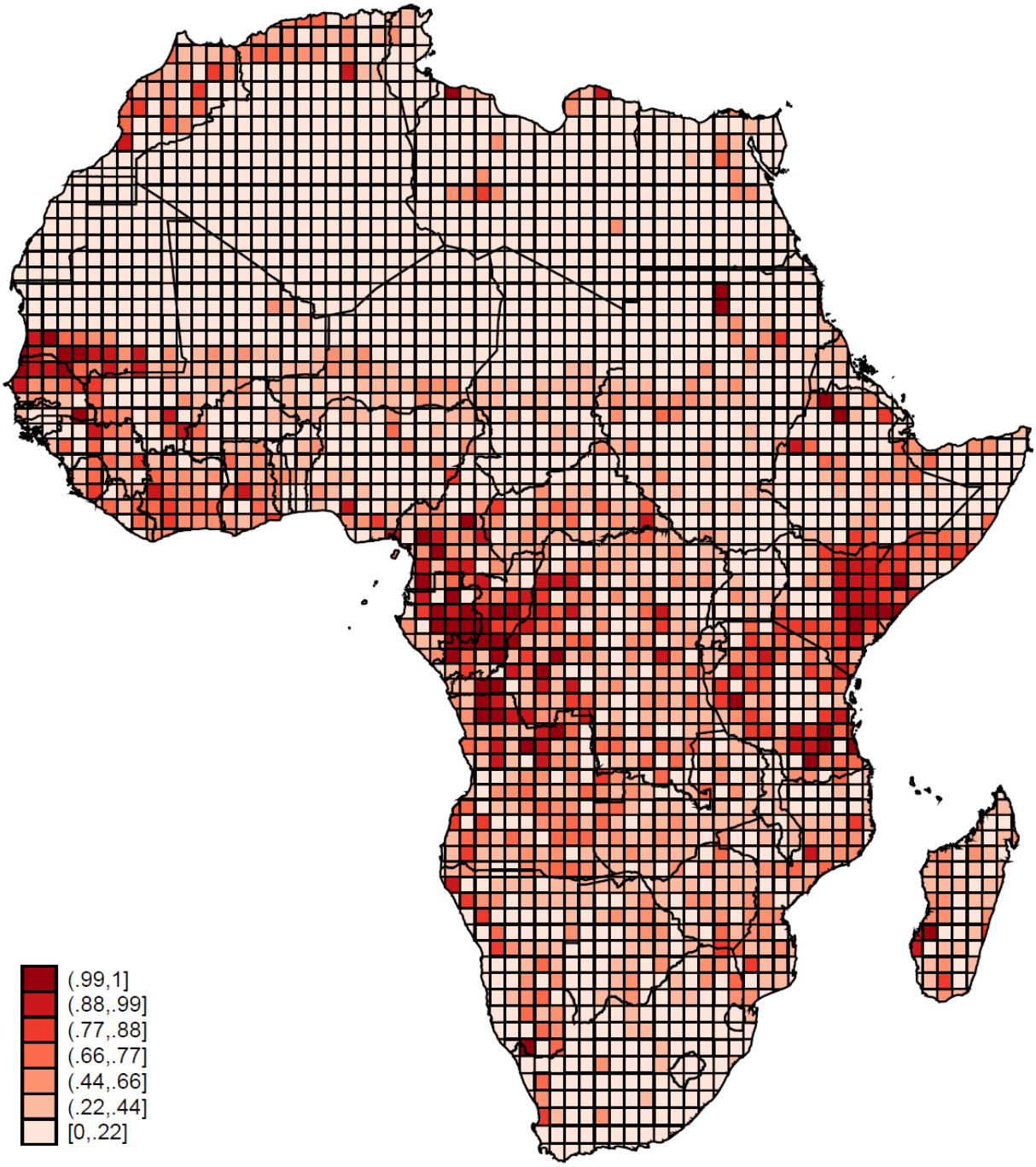

Figure 8:
Average projected SPEI Shock, 2012 – 2030

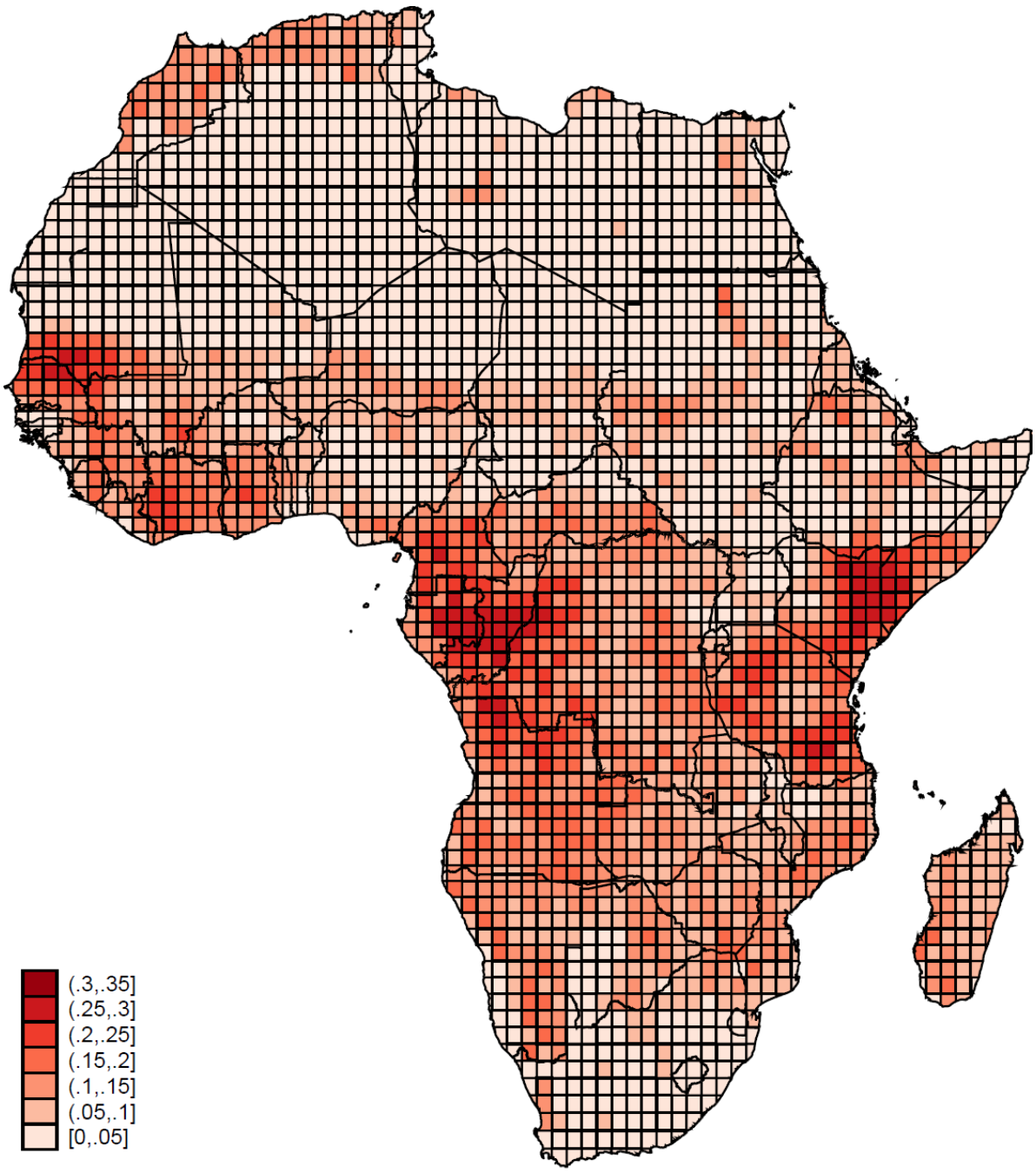

Figure 9:
Average marginal effects of SPEI Shock , projected 2012-2030

Appendix Table A1: Conflict incidence and other SPEI based climate indicators, panel

Dependent variable (Y) = 1 if conflict event in year t (ANY EVENT)

	(1)	(2)	(3)	(4)	(5)	(6)
	Standalone			**Growing Season Maincrop**		
	Model I	Model II	Model III	Model I	Model II	Model III
Y, t-1			0.334***			0.334***
			(0.0049)			(0.0049)
W · Y			0.0456***			0.0455***
			(0.0010)			(0.0010)
SPEI	0.0028	0.0235*	0.0117	0.0087	0.0223	0.0100
	(0.0056)	(0.0136)	(0.0120)	(0.0066)	(0.0142)	(0.0131)
SPEI, t-1	-0.0157***	0.0092	-0.0079	-0.0087	0.0255*	0.0107
	(0.0058)	(0.0138)	(0.0119)	(0.0071)	(0.0149)	(0.0136)
SPEI, t-2	-0.0099*	0.0038	-0.0019	-0.0019	0.0123	0.0021
	(0.0057)	(0.0138)	(0.0114)	(0.007)	(0.0152)	(0.0130)
SPEI, Growing Season Indicator				-0.0115	-0.0003	0.0009
				(0.0119)	(0.0144)	(0.0133)
SPEI, Growing Season Indicator, t-1				-0.0147	-0.0343**	-0.0384**
				(0.0123)	(0.0161)	(0.0151)
SPEI, Growing Season Indicator, t-2				-0.0168	-0.0203	-0.0106
				(0.0123)	(0.0163)	(0.0146)
W · SPEI		-0.0033	-0.0008		-0.0013	0.0005
		(0.0021)	(0.0018)		(0.0023)	(0.002)
W · SPEI, t-1		-0.004*	-0.0003		-0.0057**	-0.003
		(0.0021)	(0.0018)		(0.0024)	(0.0021)
W · SPEI, t-2		-0.0023	0.000		-0.0020	-0.0003
		(0.0020)	(0.0017)		(0.0024)	(0.002)
W · SPEI, Growing Season Indicator					-0.0036	-0.0023
					(0.0027)	(0.0023)
W · SPEI, Growing Season Indicator, t-1					0.0035	0.0057**
					(0.0029)	(0.0025)
W · SPEI, Growing Season Indicator, t-2					-0.0002	0.0009
					(0.003)	(0.0024)
Observations	37,425	37,425	37,425	37,425	37,425	37,425
R squared	0.327	0.353	0.346	0.327	0.354	0.346

Notes:

Each observation is a cell/year. All regressions include controls listed in table 2, country and year fixed effects

W = binary contiguity matrix, cutoff 180 km.

Standard errors in parenthesis. Cols. 1, 2, 4 and 5 corrected for spatial and serial correlation.

Cols. 3 and 6 corrected for clustering at the cell level. *** p<0.01, ** p<0.05, * p<0.1

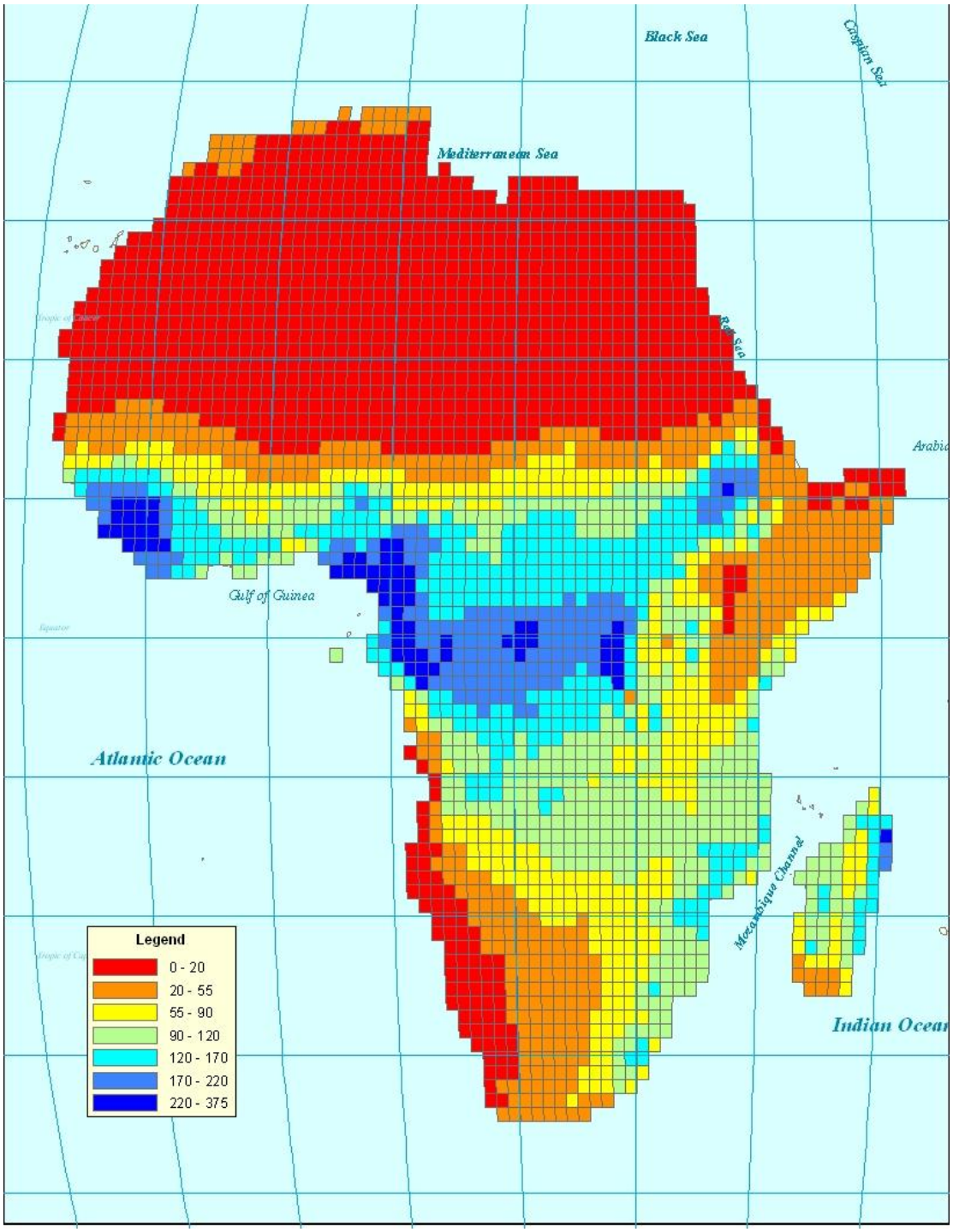

Figure A1:

Average yearly rainfall (in mm), year 2000

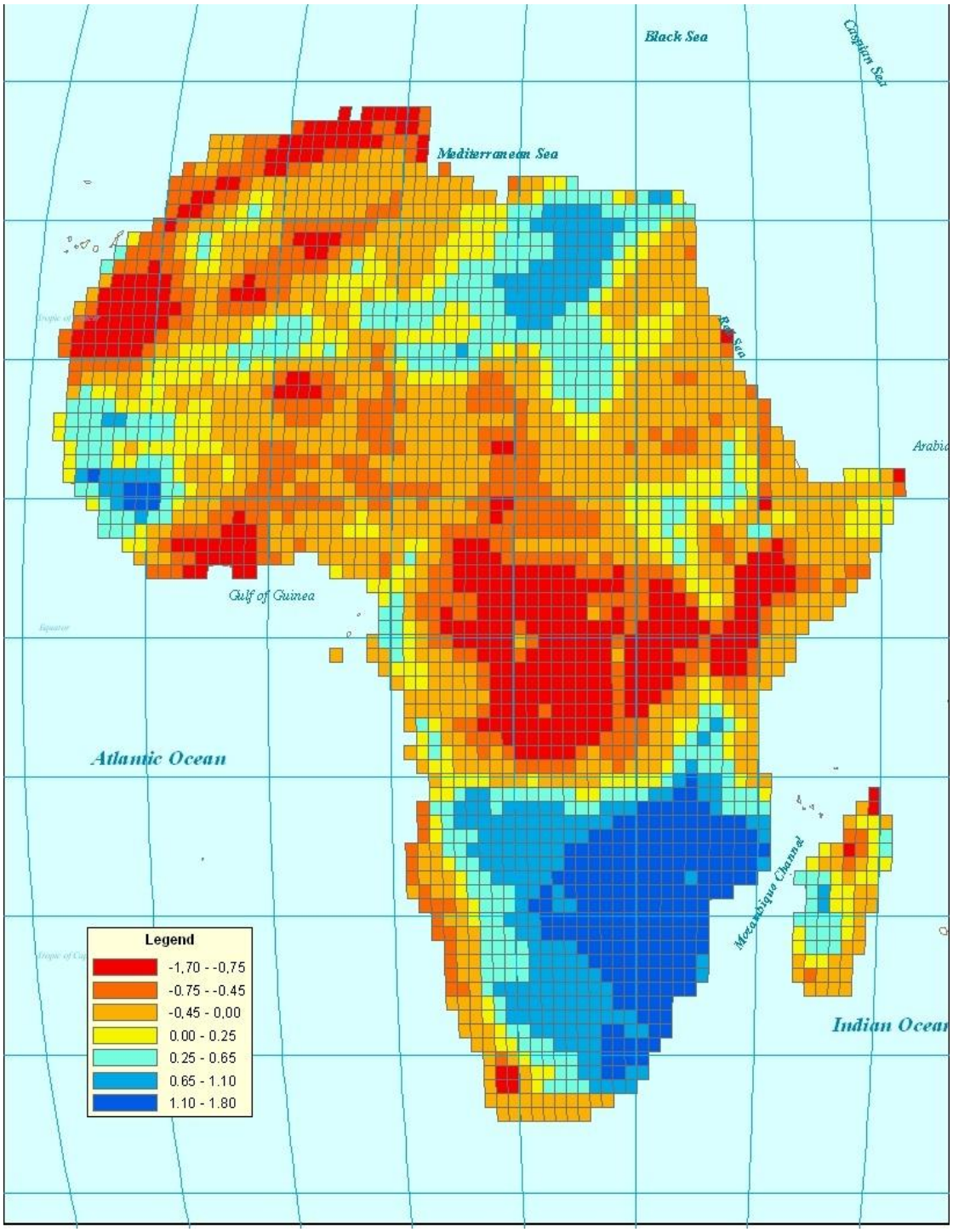

Figure A2:

SPEI, year 2000

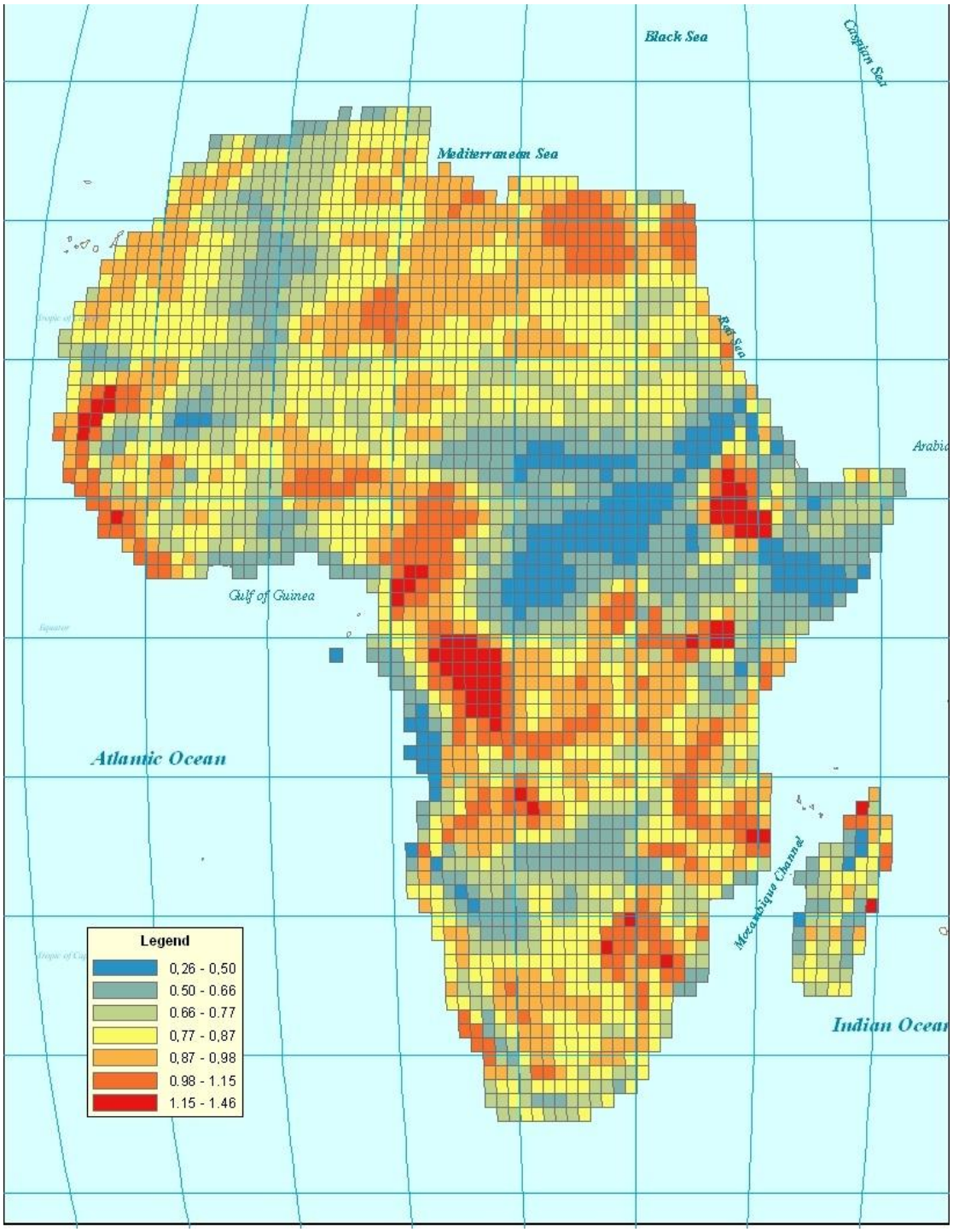

Figure A3:

Temperature, absolute deviation from cell mean, year 2000